

Report DWLBC 2004/44



action
Salinity & Water
AUSTRALIA

South Australia Salt Mapping and Management Support Project

Modelling Groundwater Salinisation in the Tintinara Highlands area of SA:

K.Osei-Bonsu, S.Barnett, F.Leaney, P.Davies

December 2004



Table of Contents

ABSTRACT.....	5
INTRODUCTION.....	6
HYDROGEOLOGY	7
GMS MODEL	8
MODEL CONSTRUCTION.....	8
MODEL CALIBRATION.....	13
STEADY STATE CALIBRATION.....	17
SENSITIVITY ANALYSIS.....	22
TRANSIENT MODEL CALIBRATION	24
MODEL VALIDATION	30
SALT LOAD MODELLING	33
STEADY STATE TRANSPORT SIMULATION	34
TRANSIENT STATE TRANSPORT CALIBRATION.....	36
SIMULATION OF GROUNDWATER SALINIZATION IMPACTS	39
CONCLUSIONS AND RECOMMENDATIONS.....	44
REFERENCES.....	45

List of figures

Figure 1	Aerial EM survey area and location of drill holes	6
Figure 2	Hydrogeological cross section	8
Figure 3	Model extent and survey area	9
Figure 4	Model grid.....	9
Figure 5	Cross section showing five model layers.....	10
Figure 6...	Boundary conditions for the MGL and RG aquifers	13
Figure 7	Recharge zones and values used in calibrating predevelopment potentiometric head	15
Figure 8	Estimated groundwater extractions from 1990/91 to 2000/01.....	16
Figure 9	Computed vs observed potentiometric surface in the MGL and RG aquifers ..	20
Figure 10	Steady state calibration results along 1:1 correlation line.....	20
Figure 11	Calibrated horizontal hydraulic conductivities for the MGL and RG aquifers	21
Figure 12	Sensitivity analysis	23
Figure 13	Location of observation wells in study area	24
Figure 14	Comparison between simulated and measured transient conditions – Bores MKN 1, 8, and 11	25
Figure 15	Comparison between simulated and measured transient conditions – Bores MCA 3, SHG 2 and 5	26
Figure 16	Comparison between simulated and measured transient conditions – Bores SHG 6 and 7	27
Figure 17	Calibrated values of specific yield (MGL) and storativity (RG).....	29
Figure 18	Comparison between simulated and measured validation conditions – Bores MKN 8 and 11, MCA3	31
Figure 19	Comparison between simulated and measured validation conditions – Bores SHG 5, 6 and 7	32
Figure 20	Steady-state simulated salinity contours	34
Figure 21	Steady-state simulated salinity contours	35
Figure 22	Comparison between simulated and measured transient salinity conditions – Bores MCA 2 and 7, MKN 2.....	37
Figure 23	Comparison between simulated and measured transient salinity conditions – Bores MKN 11 and 19.....	38
Figure 24	Modelled salinity predictions at five observation bores.....	40
Figure 26	Modelled salinity predictions at three irrigated sites.....	42
Figure 27	Modelled irrigated salinity distribution in the MGL aquifer.....	43

List of Tables

Table 1	Aquifer and confining layer hydraulic parameters from literature	14
Table 2	Comparison of measured and calculated heads	18
Table 3	Steady state calibration error summary	18
Table 4	Summary statistics for simulated horizontal hydraulic conductivity.....	22
Table 5	Sensitivity analyses with respect to horizontal hydraulic conductivity	23
Table 6.	Comparison of measured and calculated salinity	35
Table 7.	Transport parameters used in model calibration.....	35
Table 8.	Comparison of measured and calculated salinity - April 2003.....	36
Table 9	Comparison of 2004 and 2100 simulated salinity	39

ABSTRACT

Previous field investigations in the Tintinara Highlands have confirmed that groundwater salinisation will result from increased drainage following the clearing of native vegetation. The increased drainage results in subsequent leaching of saline soil water in the unsaturated zone downwards towards fresher groundwater. A lag time of approximately fifty to hundreds of years is expected before there will be observed increases in groundwater salinity. This lag time will depend on the clay content of the near surface soil, that of the soil throughout the unsaturated zone and also on the depth to groundwater. If irrigation occurs, the lag time is shortened considerably and increases in groundwater salinity may be expected within five to ten years of water being applied.

As part of the South Australian Salinity Mapping and Management Support Project funded by the National Action Plan for Salinity and Water Quality, spatial coverages were developed of the relevant parameters in the salinisation model to estimate recharge and salt flux to the aquifer over time using data collected by an airborne EM survey and drill core. This report details the construction of a groundwater model which was used to predict the impacts of the salt flux on groundwater salinity.

Under the dryland non-irrigation scenario, significant increases in aquifer salinity are predicted to occur after 50 years from the present time. Rates of increase will vary from 15 – 45 mg/L/yr, depending on soil type. These increases in groundwater salinity will result in unsuitability for new vegetable irrigation (in areas not previously irrigated), in about 50 years time. Significant areas will not have groundwater suitable for domestic consumption in about 80 years, while lucerne irrigation in new areas and stock supplies will be able to be maintained indefinitely.

Beneath irrigated areas, the flushing of salt is accelerated markedly, with increases in salinity beneath the irrigated area beginning after only 10 years, with salinities too high for use after a further five years in areas of high recharge with sandy soils. Obviously, clayey soils and rotation of irrigated areas will delay salinity impacts by up to 30 to 40 years. After 50 years, the maximum lateral movement of salinised groundwater to the west from beneath the irrigated areas is about 500 m.

Before management strategies are investigated, salinity responses to varying irrigation drainage rates should be modeled to simulate the variation in irrigation efficiencies under different crop types. Regular salinity monitoring of all irrigation bores and some dryland stock bores should be continued to help validate the model and better calibrate some parameters.

INTRODUCTION

Over the last five years, there have been several field investigations in the Tintinara Highlands which were carried out to provide a time frame for groundwater salinisation in areas cleared of native vegetation and in areas that have subsequently undergone irrigation development or in areas where irrigation is planned for the future (Leaney et al., 1999, Leaney, 2000, Leaney, 2001). During these initial projects, unsaturated zone/groundwater models were developed to determine the rate of groundwater salinisation in cleared and irrigated areas. The initial projects also included field investigations to collect data for these models.

Results from these initial investigations suggested that, in cleared areas, there would be a lag time before groundwater salinity would start to increase. The lag time would vary from ~50 to hundreds of years depending on the clay content of both the near surface soil and that of the soil throughout the unsaturated zone. It would also depend on the depth to groundwater. The development of higher drainage rates beneath irrigated areas would accelerate the salinisation process, and it was predicted that changes in groundwater salinity would occur in some areas within 5-10 years of the commencement of irrigation.

A limitation of these earlier studies in this area was that rates of groundwater salinisation could only be assigned to the sites that were selected for soil sampling. with no risk map for the area able to be developed.

As part of the South Australian Salinity Mapping and Management Support Project funded by the National Action Plan for Salinity and Water Quality, Leaney et al (2004) developed spatial coverages of the relevant parameters in the salinisation model to estimate recharge and salt flux to the aquifer over time using data collected by an airborne EM survey and drill core (Fig. 1).

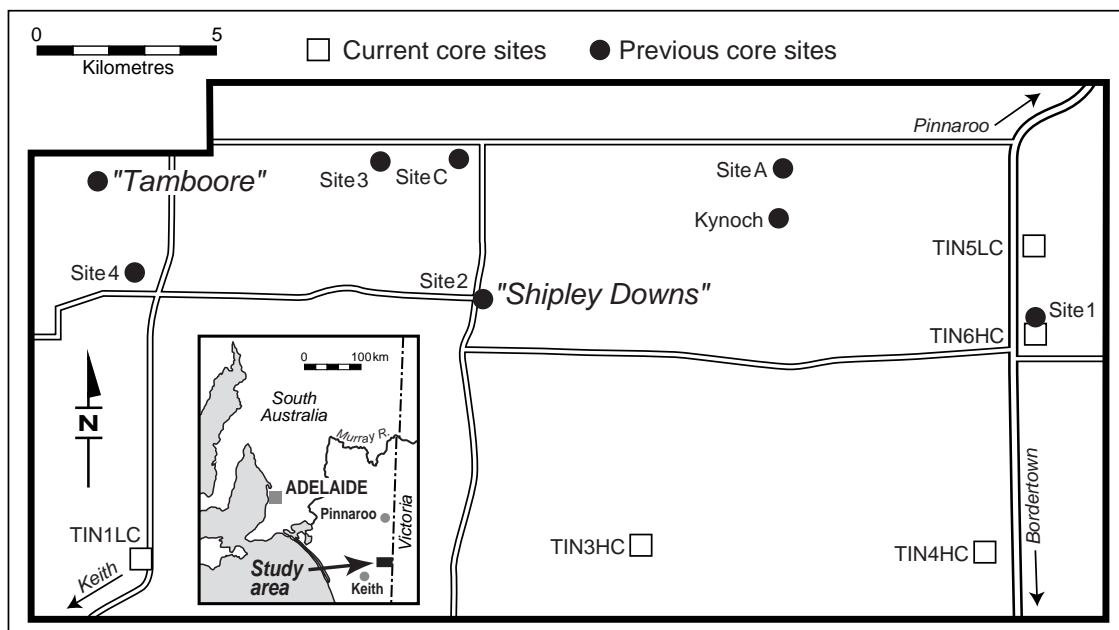


Figure 1 Aerial EM survey area and location of drill holes

Improvements to the unsaturated zone recharge and salinisation models used in earlier work were also made. This study confirmed the range in rates of salinisation that have previously been suggested for the area, and provided salt flux maps which identified areas at risk of groundwater salinisation.

This report details the construction of a groundwater model which was used to predict the impacts of the salt flux on groundwater salinity and to assist in formulating management strategies to minimise the impacts.

HYDROGEOLOGY

The study area is located in the southwestern Murray Basin. There are three main aquifers separated by two confining layers. Figure 2 shows the regional hydrogeology along an east-west section through the Mallee region to the north of the study area. These aquifers are, in order of increasing depth below the surface :

- **Pliocene Sands aquifer:-** comprising the Loxton – Parilla Sands which underlie almost all of the study area and ranges from 10 to 30 m in thickness, it forms an unconfined aquifer which is saturated only in Victoria to the east. The unit consists of unconsolidated to weakly cemented fine to coarse sand, with some clayey layers.
- **Bookpurnong Beds (confining layer):-** this unit occurs only in the eastern part of the area where it dips down gradually to the east and increases in thickness to about 25 m. It consists of poorly consolidated plastic silts and shelly clays, which confines the underlying limestone aquifer. It does not occur beneath the study area.
- **Quaternary limestone aquifer:-** this permeable limestone exists only in the low-lying southwest area outside the study area, but is hydraulically continuous with the Murray Group Limestone.
- **Murray Group Limestone aquifer:-** comprises a consolidated, highly fossiliferous, fine to coarse limestone, which is the aquifer developed for irrigation in the study area and is unconfined over most of the modelled area, except for the eastern part where it is confined. It thickens to the northeast from about 75 to 95 m.
- **Ettrick Formation (confining layer):-** a low permeability layer between the Murray Group Limestone and the underlying confined aquifer, consisting of a glauconitic and fossiliferous marl varying between 10 and 25 m in thickness;
- **Renmark Group aquifer:-** a confined aquifer underlying the whole region, it comprises unconsolidated carbonaceous sands, silt and clay up to 150 m thick which directly overlie basement rocks.

Within the study area, groundwater flow in the both the unconfined Murray Group Limestone and confined Renmark Group aquifers, is from east to west. The depth to the watertable in the limestone aquifer varies from 10 m in the southwest, to 60 m in the northeast.

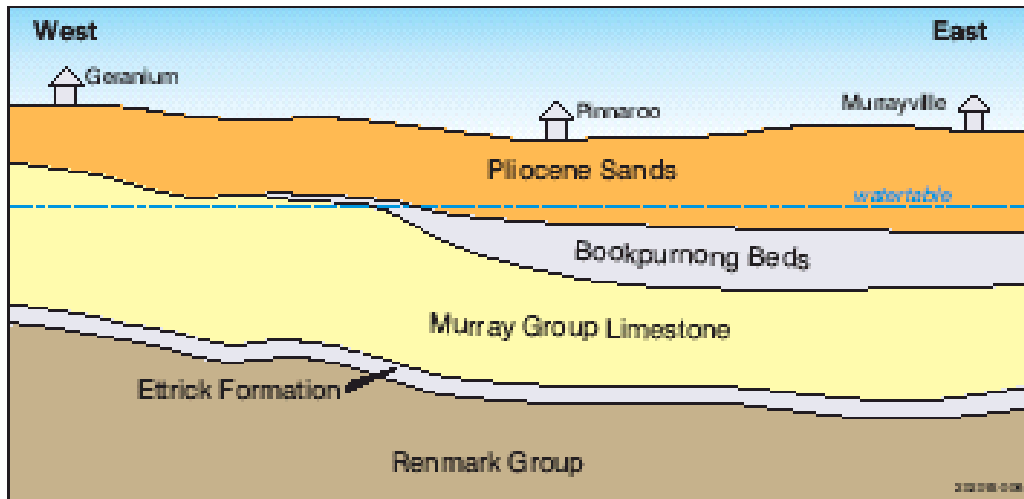


Figure 2 Hydrogeological cross section

GMS MODEL

The groundwater flow system of the study area was numerically simulated in three dimensions using MODFLOW within a GMS platform. GMS is a comprehensive MODFLOW interface that provides tools for every phase of groundwater simulation including site characterisation, model development, post-processing, calibration and visualization. With GMS, models can be defined and edited at conceptual model level or on a cell-by-cell basis at the grid level. In addition to MODFLOW, GMS has interfaces to solute transport and particle tracking models (MODPATH, MT3DMS, RT3D, and VS2D).

MODFLOW is a widely used modular finite-difference model that simulates the flow of groundwater of uniform density (McDonald and Harbaugh, 1988). MODFLOW solves the 3-D partial differential equation of groundwater flow with an implicit finite difference scheme in rectangular coordinates.

MODEL CONSTRUCTION

Because the model is also going to be used for groundwater management issues, the extent is much larger than the aerial survey area (Fig. 3). The model area was represented horizontally on a 2-D grid (Fig 4) and extends 200 km east to west, and 200 km north to south. The AMG co-ordinates of the model domain are Easting 336 433 – 536 433 and Northing 5942 682 – 6142 682. The modelled area was discretized into 109 rows and 128 columns, with the horizontal grid spacing varying from 600 m to 2000 m, with finer discretization in the study area.

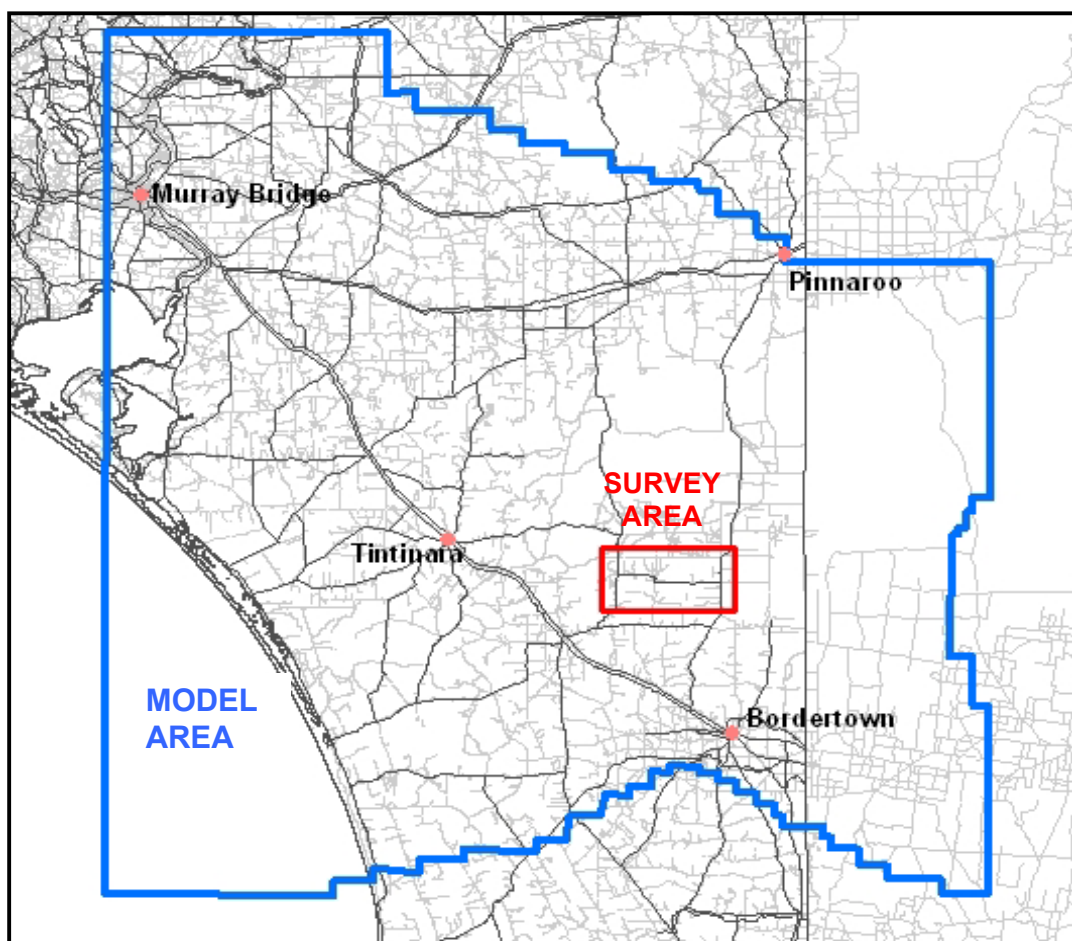


Figure 3 Model extent and survey area

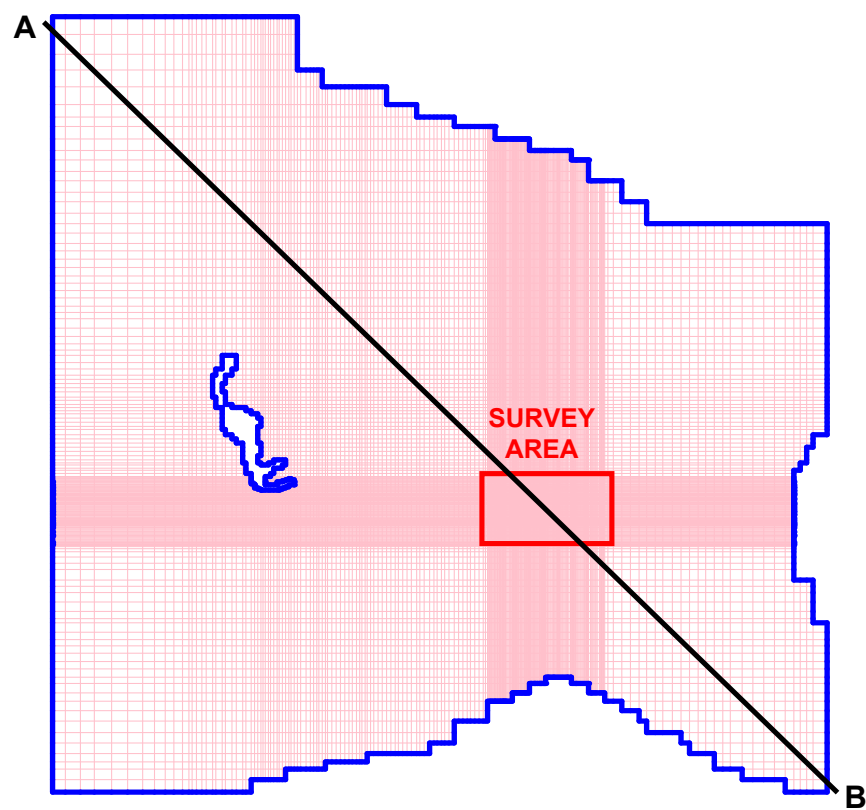


Figure 4 Model grid

Three kinds of boundary conditions were used in modelling the groundwater flow regime of the study area. The areal boundaries of the model were either fixed head, no flow or general head boundaries, and were based on the predevelopment water level maps.

Vertically, the model was conceptualised with five layers as follows. Figure 5 presents a cross section through the model area depicting these five layers. The location of the section is shown in Figure 4.

Layer 1 - Pliocene Sands Aquifer (PS)

Although it forms a thin unconfined aquifer in the east, it was considered superfluous for this modeling exercise, and consequently this layer was made inactive which still allowed vertical recharge down to the limestone aquifer.

Layer 2 - Bookpurnong Beds confining layer (BB)

A low permeability layer found only in the east, and as only very low volumes of water flow in and out from this layer, no flow boundaries surround the model edges.

Layer 3 - Murray Group Limestone Aquifer (MGL)

An unconfined aquifer over most of the model (confined only in the east), where the northern, eastern and southern edges of the model area were assumed to be no flow boundaries as they are parallel to groundwater flow (Fig. 6). The western boundary along the coast and the River Murray is a fixed head boundary, with fixed head cells in the southeast corner representing lateral flow into the model area from recharge areas to the southeast. A general head boundary is applied in the northeast corner to allow flow out of the model toward the river.

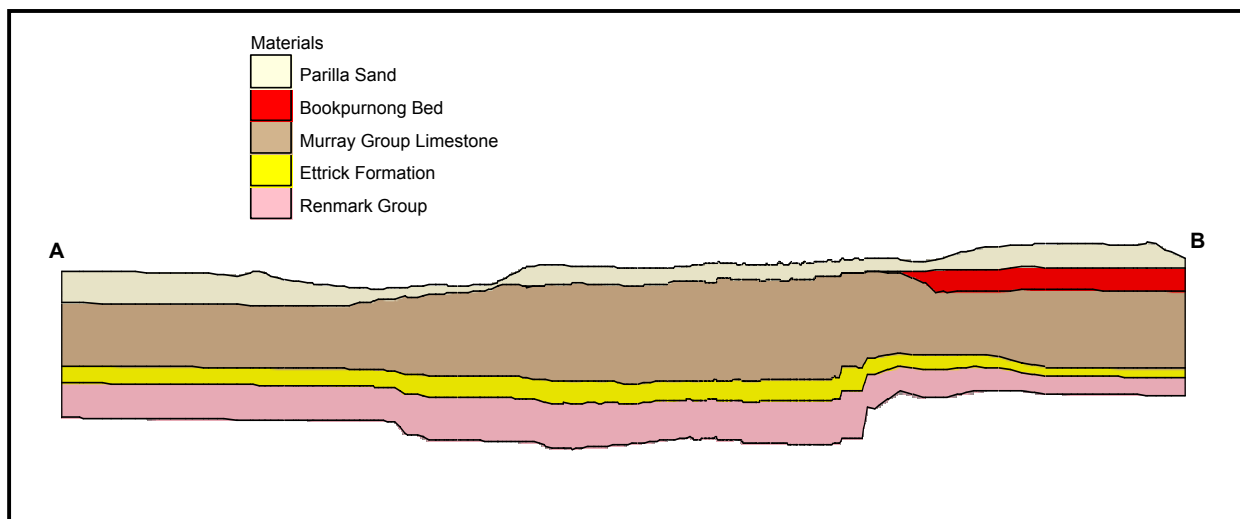


Figure 5 Cross section showing five model layers

Layer 4 - Ettrick Formation confining layer (EF)

A low permeability layer, and as only very low volumes of water flow in and out from this layer, no flow boundaries surround the model edges.

Layer 5 - Renmark Group Aquifer (RG)

A confined aquifer over all of the model area, where the northern, eastern and southern edges of the model area were assumed to be no flow boundaries as they are parallel to groundwater flow (Fig. 6). The western boundary at the coast is a fixed head boundary, with fixed head cells in the southeast corner representing lateral flow into the model area from recharge areas to the southeast. A general head boundary is applied in the northeast corner to allow flow out of the model toward the river. A no flow boundary applies to the base of the aquifer to represent impermeable weathered basement.

The ground surface elevation, the top and bottom elevations of all aquifer layers and confining beds, and the basement elevation were all specified and based on structure contours available from the Murray Basin Hydrogeological Map series. In some areas, this data has been heavily modified to reflect more recent drilling and some new interpretations of borehole logs.

Model assumptions

The following assumption were made in the conceptualisation of the groundwater flow system:

- The aquifers are assumed to be porous media
- Flow in the confining beds is vertical and represents leakage between the aquifers
- There is very little vertical or horizontal movement of groundwater in the basement rock and consequently, it was modelled as no-flow boundary
- The flow within the aquifers is horizontal
- All horizontal flows enter or leave the MGL and the RG aquifers only
- Groundwater moves radially outwards from the southeast corner in the study area towards the northwest and north-northwest and towards the west
- The flow in the portion of the MGL and the RG aquifers lying between the northern boundary of the model area and the Murray River is strongly controlled by the river elevation.

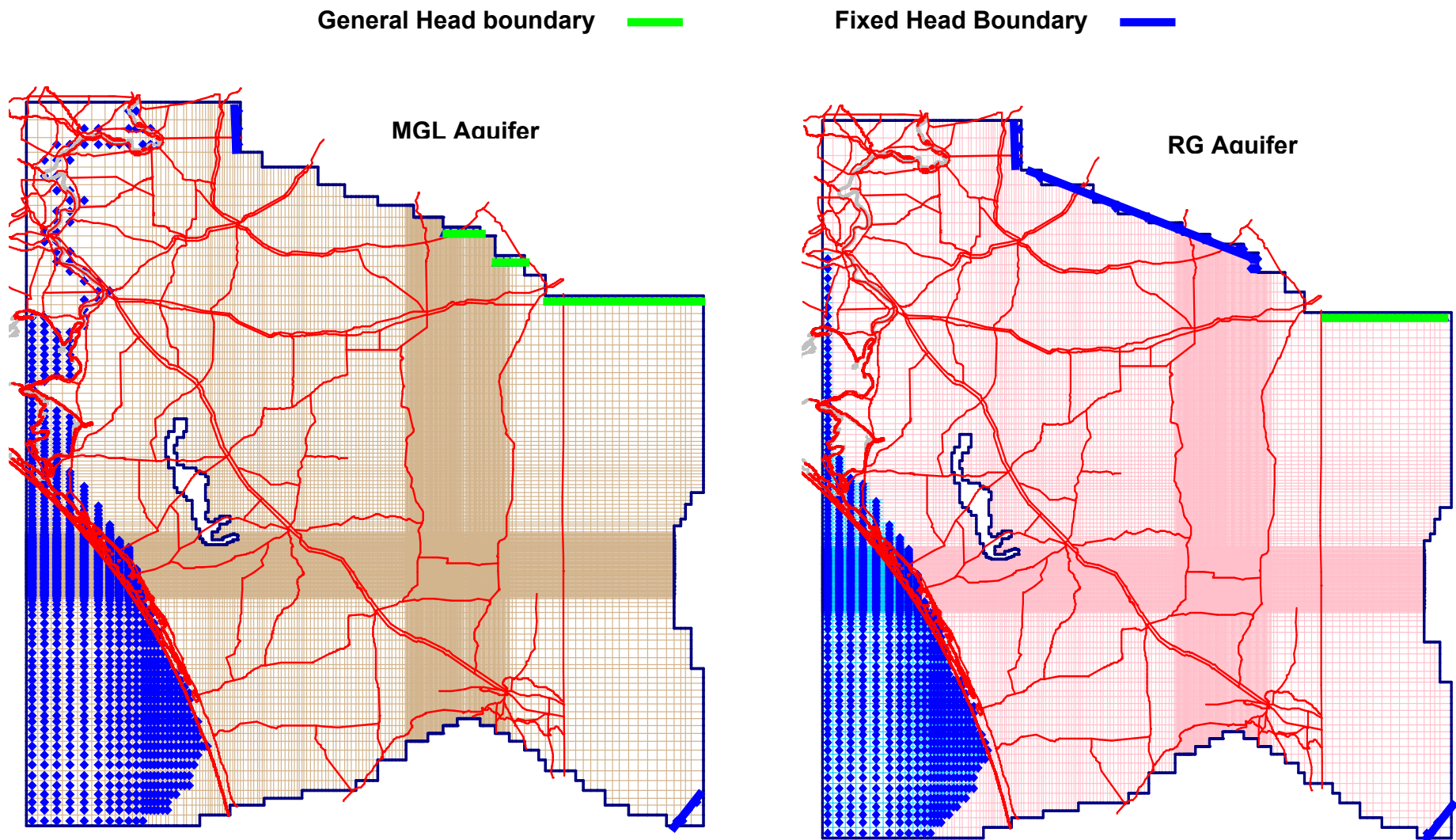


Figure 6... Boundary conditions for the MGL and RG aquifers

MODEL CALIBRATION

The groundwater flow modelling undertaken for this study involves the following steps:

- Establishing the initial conditions (hydraulic parameters, recharge, pumping etc)
- Carrying out a steady state simulation to represent predevelopment groundwater levels in the aquifer system
- Using the simulated steady state groundwater levels as initial conditions for a transient state calibration
- Using the calibrated transient state model to assess the groundwater level and salinity response of the MGL aquifer to groundwater development and changes in land use (clearing) in the future.

Initial conditions

Reported aquifer properties and hydraulic stresses were initially used as input parameters. In order to match observed heads to computed heads, these initial input parameters were modified during model calibration.

Aquifer hydraulic parameters

The initial aquifer properties, such as horizontal hydraulic conductivity, vertical hydraulic conductivity, specific yield, specific storage and anisotropy used in the model were sourced from published and unpublished reports. These values are presented in Table 1. The initial hydraulic parameters used in the model were selected from these values. The degree of anisotropy K_x / K_z reported in the literature from aquifer tests is 20:1 (Lawrence, 1975). The initial conductances for general-head-boundary cells were calculated using cell size, layer thickness, horizontal hydraulic conductivity and distance of the cell from the Murray River.

Recharge

Recharge to the aquifer from rainfall varies spatially and temporally, and is dependent on soil type, topography and changes in land-use. Recharge rates for uncleared areas with deep-rooting vegetation, like mallee, are generally believed to be less than 1 mm/yr (Leaney et al, 1999). In areas with clayey surface soils, recharge may be less than 0.1 mm/yr, while in areas with sandy surface soil recharge rates are highest. The initial recharge values used in calibrating the steady state model were obtained from Leaney et al (2004) and are shown in Figure 7.

Recharge, which was applied to the top active layer at each cell, was simulated using the RCH module in MODFLOW. The RCH module simulates constant rates of recharge for each stress period. Recharge during predevelopment was assumed to equal the long-term average recharge, and it was assumed that recharge remained constant at the values shown in Figure 7 until after 1960 when land clearing started.

Table 1 Aquifer and confining layer hydraulic parameters from literature

Layer	Location	Aquifer transmissivity (m ² /d)	Horizontal hydraulic conductivity (m/d)	Specific yield/ Storativity	Source
Pliocene Sands	-	-	2.3	-	Lawrence, 1975
	Loxton Berri-Barmera	10 – 75 40 - 120	0.5 – 2.5 (fine sand) 2 – 6 (coarse sand)	0.1 – 0.2	Barnett, 1991
Bookpurnong Beds	-	-	4.67x10 ⁻⁴	-	Lawrence, 1975
Murray Group Limestone	Parilla	602	-	-	Lawrence, 1975
	Waikerie – Overland Corner	120 - 200	1.5 – 2.5	0.02 – 0.06	Barnett, 1991
	Waikerie	1.5 – 120	-	-	Lawrence, 1975
	Wanbi	265 – 330	3.9 – 10.7	2.5x10 ⁻³	Lawrence, 1975
	Morgan-Purnong	20 - 150	1 - 3	0.1 – 0.2	Barnett, 1991
	Blanchetown-Purnong	10 - 100	1 - 2	0.1 – 0.2	Barnett, 1991
	Naracoorte Limestone	255 – 1800	-	-	Lawrence, 1975
	Gambier Limestone	4040	-	-	Lawrence, 1975
Ettrick Formation	-	-	2.63x10 ⁻³	-	Lawrence, 1975
Renmark Group	Keith (TWS 3B)	0.545	6.05	-	Lawrence, 1975
	Keith (TWS 7)	0.40	2.31	-	Lawrence, 1975
	Naracoorte	1240	-	-	Lawrence, 1975
	Regional	30 - 3500	1 – 5 (Olney Fm) 5 – 10 (Warina Sand)	2x10 ⁻⁴	Barnett, 1991

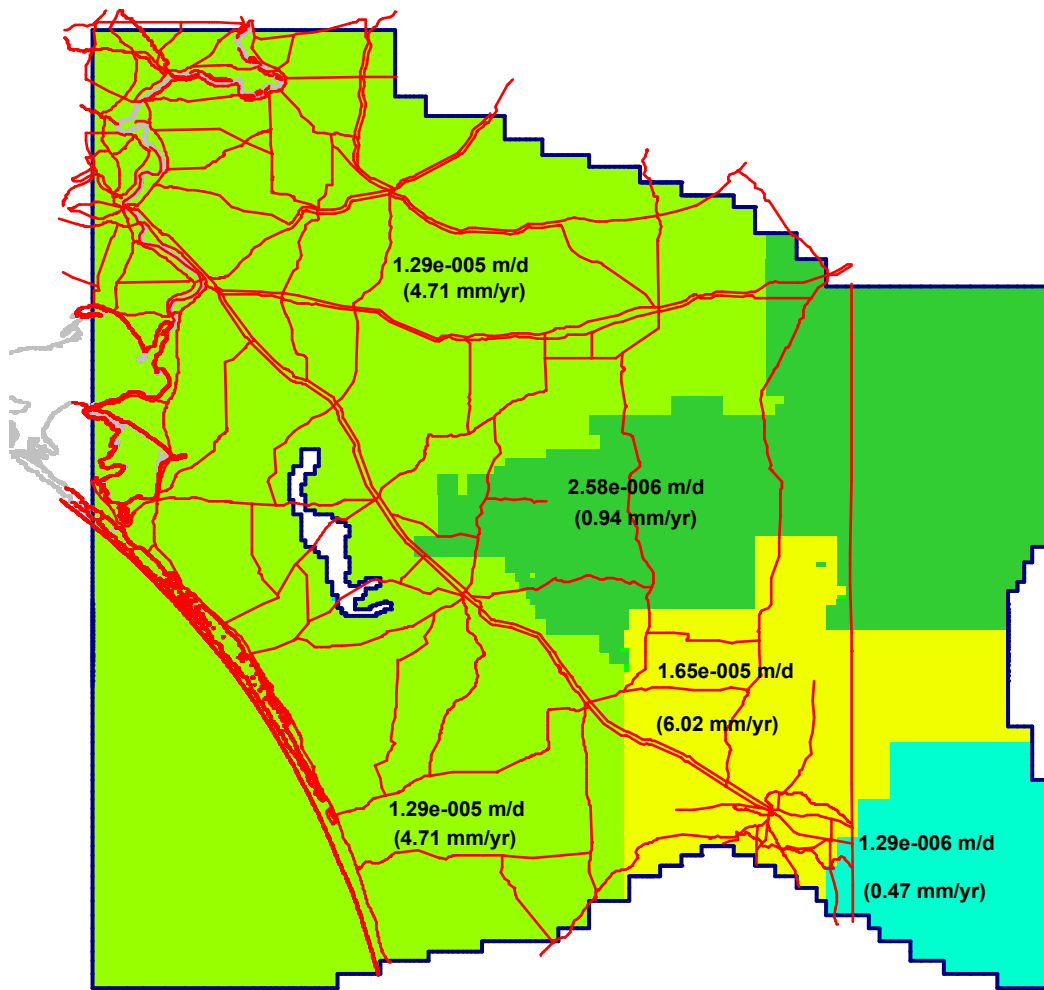


Figure 7 Recharge zones and values used in calibrating predevelopment potentiometric head

Groundwater extraction

The groundwater resource is developed for irrigation, stock and domestic purposes. Estimated extraction volumes from the aquifers since 1990 in the modelled area are presented in Figure 8, and have increased from 5436 ML in 1990/91, to 19 684 ML in 2000/01. Most extraction is from the MGL aquifer, which currently provides about 88.5% of the total usage. Within the smaller study area, estimated extractions increased from 120 ML to 5135 ML over the same period.

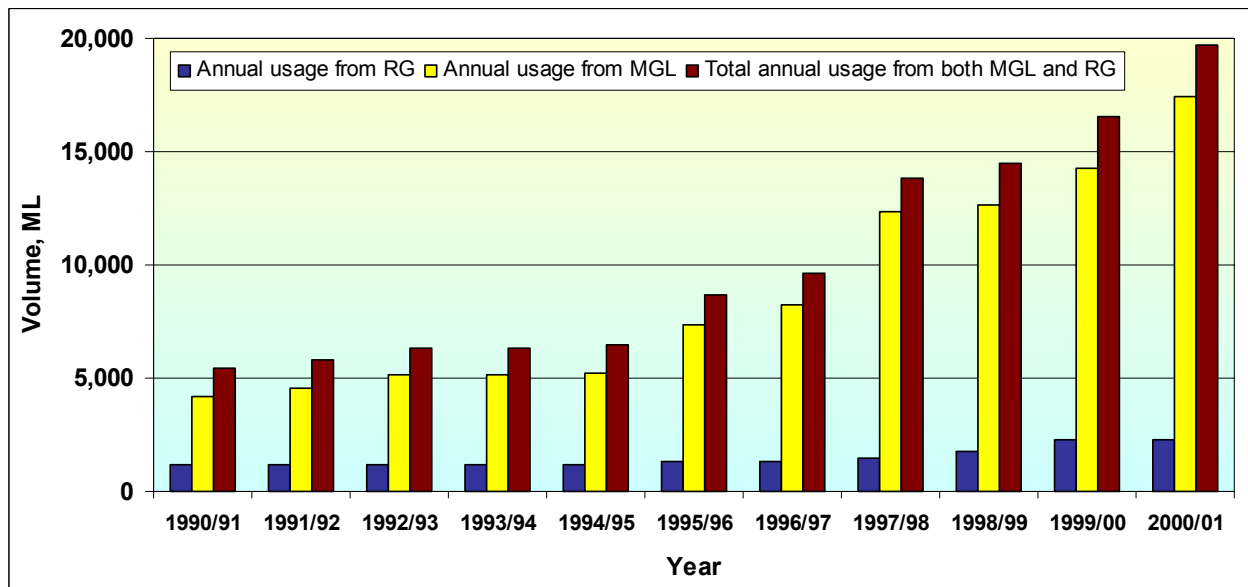


Figure 8 Estimated groundwater extractions from 1990/91 to 2000/01

Groundwater pumping rates were simulated using the WEL module in MODFLOW, which simulates constant rates of well discharge for each stress period. Pumping rates were assigned to the node of each model cell in which a pumping well is located. If multiple wells were pumping from the same model cell, pumping rates were combined. Figure... shows the location of the extraction wells.

Historical Water Levels

Predevelopment water levels in the study area were obtained from published maps (Barnett 1991, Kellett et al 1990). Regular monitoring of water levels in the study area started in 1983. Compared to the predevelopment conditions, water levels in the MGL in the study area are rising and in 2004, were between 0.5 to 1.5 m higher than 1983.

Calibration

The model was calibrated in a steady-state mode with predevelopment water levels (prior to 1960) and in transient (time varying) mode with water levels from 21 observation wells measured between 1983 and 2004. Both the steady and transient state groundwater flow models were calibrated by using a trial-and-error method in adjusting the input hydraulic parameters and boundary conditions to obtain a best match between simulated hydraulic heads and measured water levels. The results of the calibration were evaluated both qualitatively, by comparison of contour maps and hydrographs of measured and computed heads, and quantitatively by scatter plot of inferred or measured and computed heads.

Three different error statistics were used to quantify the average error in the steady state calibration; the Mean Error (ME), the Mean Absolute Error (MAE), and the Root-Mean Square Error (RMSE). The ME is simply the average of the differences between inferred or observed and simulated heads; the MAE is calculated by taking the average of the absolute values of the differences between inferred or observed and simulated heads, and

the RMSE is calculated by taking the square root of the average of the squared differences. The plot of inferred or measured against simulated heads and water levels was also used to evaluate the degree of errors in the calibration.

The steady state model was developed first, and provided the initial conditions for the transient simulations. The transient flow model represents the stresses of pumping and considers the effects of time and changes in groundwater storage. The steady state model was calibrated to simulate the groundwater flow regime in the aquifer system prior to 1960, before the beginning of clearing in the study area. It was assumed that before 1960, there was little vegetation clearance and the aquifer system was in its natural predevelopment state in which the water levels were essentially stable and there were no significant changes of groundwater storage.

Due to the limited definition of steady state conditions on which to base the calibration of the steady state model, it was assumed that the steady state model simulates the average of long term, equilibrium conditions that are inferred to have existed prior to 1960. The steady state model was calibrated principally against potentiometric surfaces drawn, independently of the modelling exercise, to represent the average predevelopment conditions, based on published water level contour maps. The hydraulic conductivity and general head boundary conductance data were calibrated during the steady state run, while the storage coefficient data were calibrated during transient runs. The initial conductances for general head boundary cells were calculated using layer thickness, cell size and simulated hydraulic conductivities. Because recharge and pumping rates were considered known components, none of these data sets were modified during the calibration processes.

The transient state model was calibrated and validated against hydrographs of water levels in observation wells dating from 1983 to 2004. The transient model was calibrated to simulate the response of the groundwater flow regime to groundwater extraction and increase in recharge as result from land clearance.

STEADY STATE CALIBRATION

The steady state model was calibrated by trial-and-error adjustment of hydraulic conductivity values and boundary conditions until potentiometric heads matched predevelopment water levels and inferred heads at 21 observation well locations located throughout the model area. Of the 21 observation wells, 14 monitor the MGL aquifer and 7 monitor the RG aquifer. The calculated water-level elevations at each of the 21 observation well locations for the calibrated steady-state model are shown compared with the inferred (extrapolated) values in Table 2. Inferred water levels at observation well locations were used in evaluating the error statistics associated with the calibrated steady state model.

Table 2 Comparison of measured and calculated heads

Observation well	Aquifer monitored	Observation well location		Pre-development Head (m AHD) (inferred from predevelopment potentiometric surface)		
		Easting	Northing	Measured (inferred)	Calculated	Residual
ARC007	MGL	433417	6017227	22.360	22.315	0.045
CMB006	MGL	424787	6030505	19.350	19.224	0.126
CMB009	MGL	421766	6027300	17.600	17.755	0.155
CMB014	RG	430956	6025009	21.940	22.132	0.192
CMB017	RG	422358	6022292	17.950	17.996	0.046
CMB019	RG	417273	6018488	16.150	16.036	0.114
CMB026	RG	428252	6019520	19.750	19.644	0.106
DAY001	MGL	457882	6079094	41.128	41.140	0.012
LEW003	RG	417914	6036849	19.500	19.255	0.245
LEW006	MGL	420884	6038600	16.200	16.080	0.120
MCA003	MGL	465046	6022000	50.568	50.404	0.143
MKN001	MGL	456572	6020178	45.400	45.393	0.007
MKN008	MGL	452670	6020725	42.800	42.591	0.159
MNK011	MGL	456572	6020178	42.250	42.199	0.051
MKN014	MGL	455167	6023814	45.480	45.246	0.233
MKN017	MGL	459525	6023149	47.830	47.532	0.168
PNN002	RG	478717	6060956	48.220	48.232	0.012
SHG002	MGL	494530	6017748	63.380	63.166	0.214
SHG005	MGL	479081	6017500	57.400	57.223	0.117
SHG006	RG	481437	6036200	54.560	54.826	0.226
SHG007	MGL	481559	6036215	55.900	56.682	0.068

Inferred water levels and simulated hydraulic heads for predevelopment are plotted along 1:1 correlation line as shown in Figure 10. The distribution of the Mean Error, Absolute Error and Root Mean Square Error in the calibrated steady state model is shown in Table 3. After calibration, the simulated head were within 0.007 to 0.626 m of inferred water levels with Root-Mean-Square Error of 0.149 m and Mean Error of -0.062 m. The negative value for Mean Error indicates that the simulated values of head generally were lower than the inferred values of head. Comparison of simulated water levels with predevelopment water levels for the aquifers are shown in Figure 9.

Table 3 Steady state calibration error summary

Model Layer	Mean Error (m)	Mean Absolute Error (m)	Root Mean Square Error (m)
MGL	-0.096	0.120	0.139
RG	0.007	0.140	0.167
Overall	-0.062	0.127	0.149

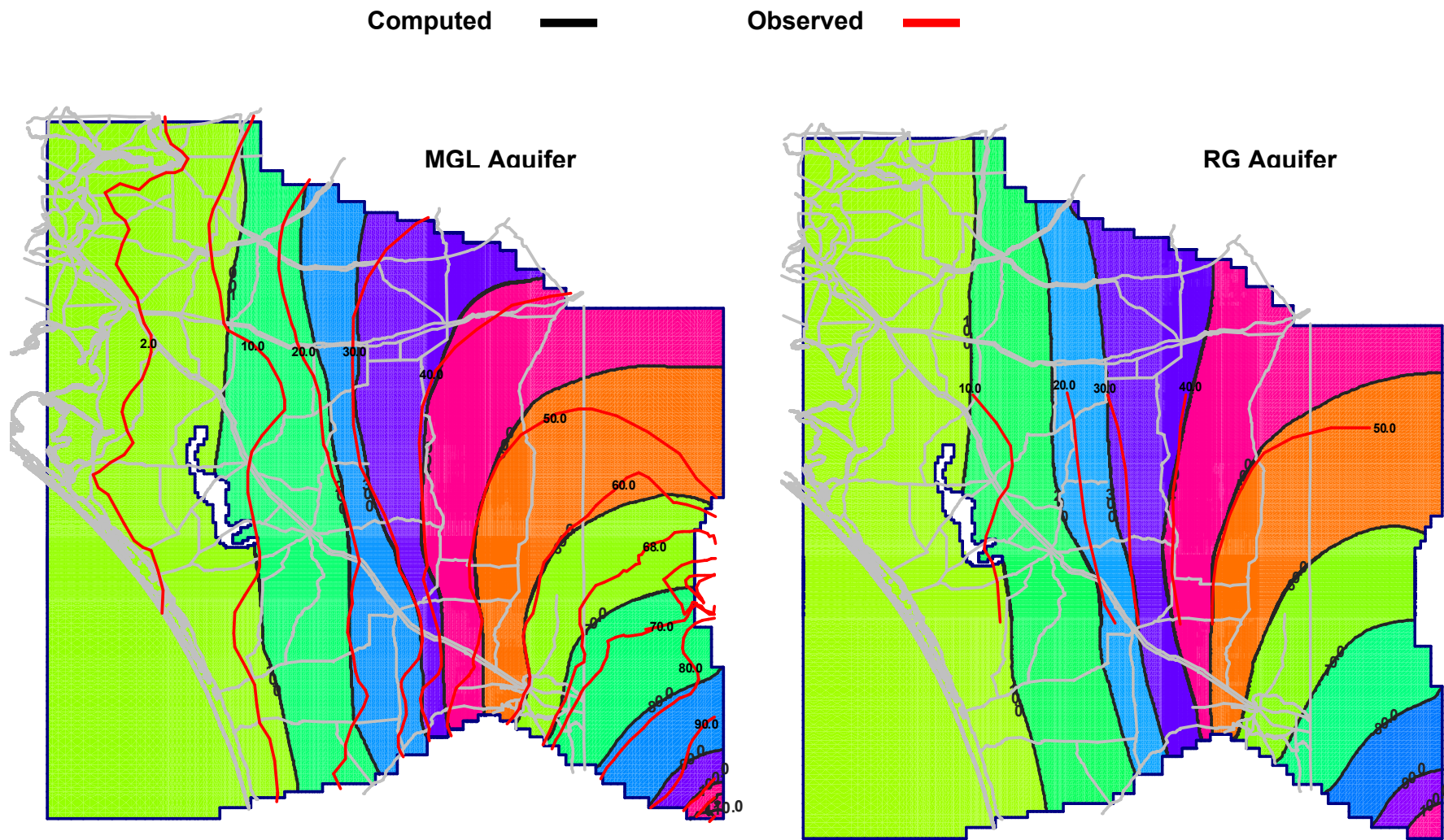


Figure 9 Computed vs observed potentiometric surface in the MGL and RG aquifers

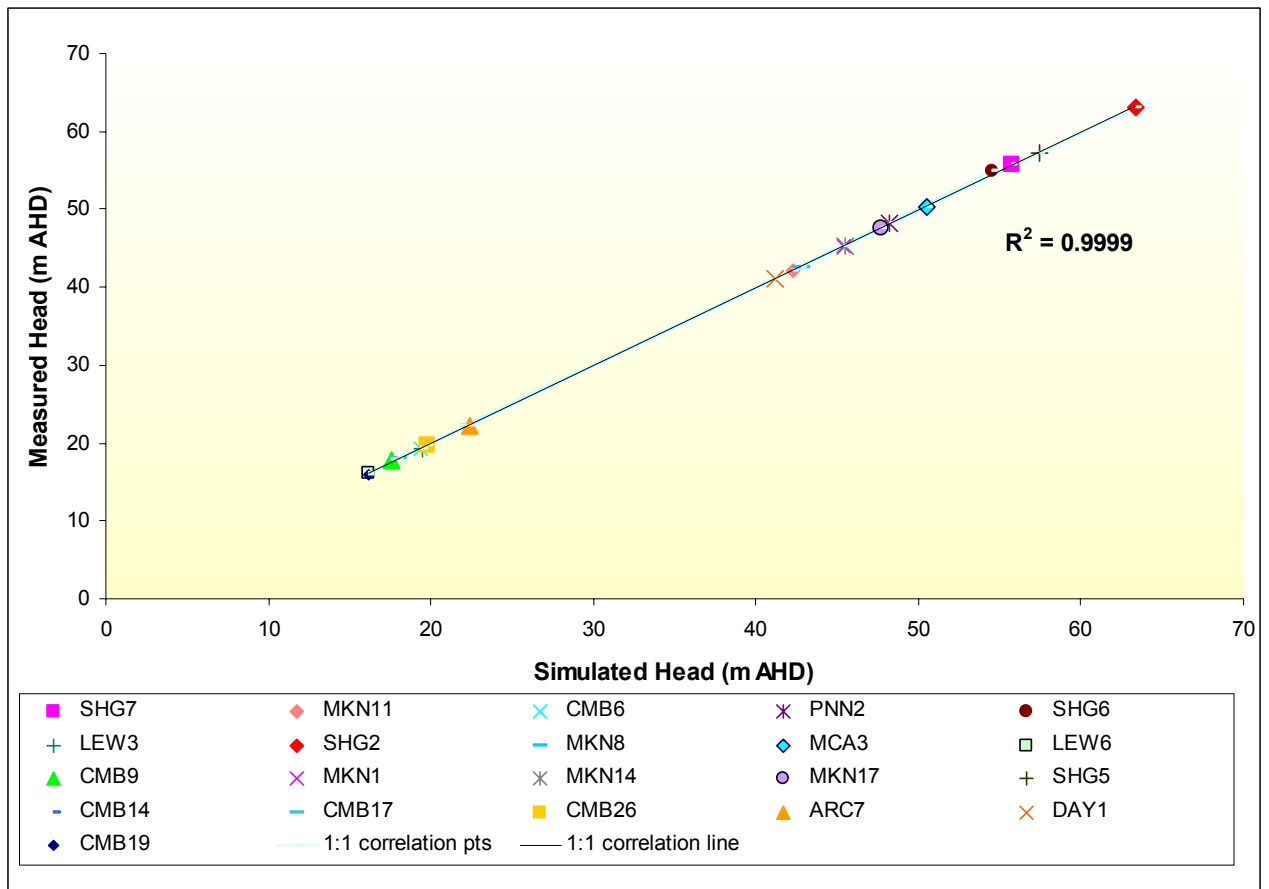


Figure 10 Steady state calibration results along 1:1 correlation line

The calibration of the flow model was focused on adjustment of hydraulic conductivity values, based on the assumption that uncertainties in the recharge rate were small relative to uncertainties in hydraulic conductivities. The calibration of the flow model used an iterative process that begins with a range of possible aquifer hydraulic values. This range (given in Table 1) is derived from pumping test data. The initial horizontal hydraulic conductivity values were revised within a reasonable range through a series of model runs until the calibration met a criteria that was based on 3 calibration statistics: (1) residual mean error of $\leq \pm 0.10$ m; (2) mean absolute error of ≤ 0.30 m; and (3) root mean square error of ≤ 0.30 m.

Once all the criteria were satisfied, and values of the hydraulic conductivity were within a reasonable range, the model was considered calibrated and the input values accepted. Figure 11 shows the horizontal hydraulic conductivity values used in the model and the basic calibration statistics are provided in Table 4. These statistics, coupled with the calibration results shown in Figure 10 and Table 3 and reported hydraulic conductivity values in the literature, indicate that the conductivity values are quite reasonable.

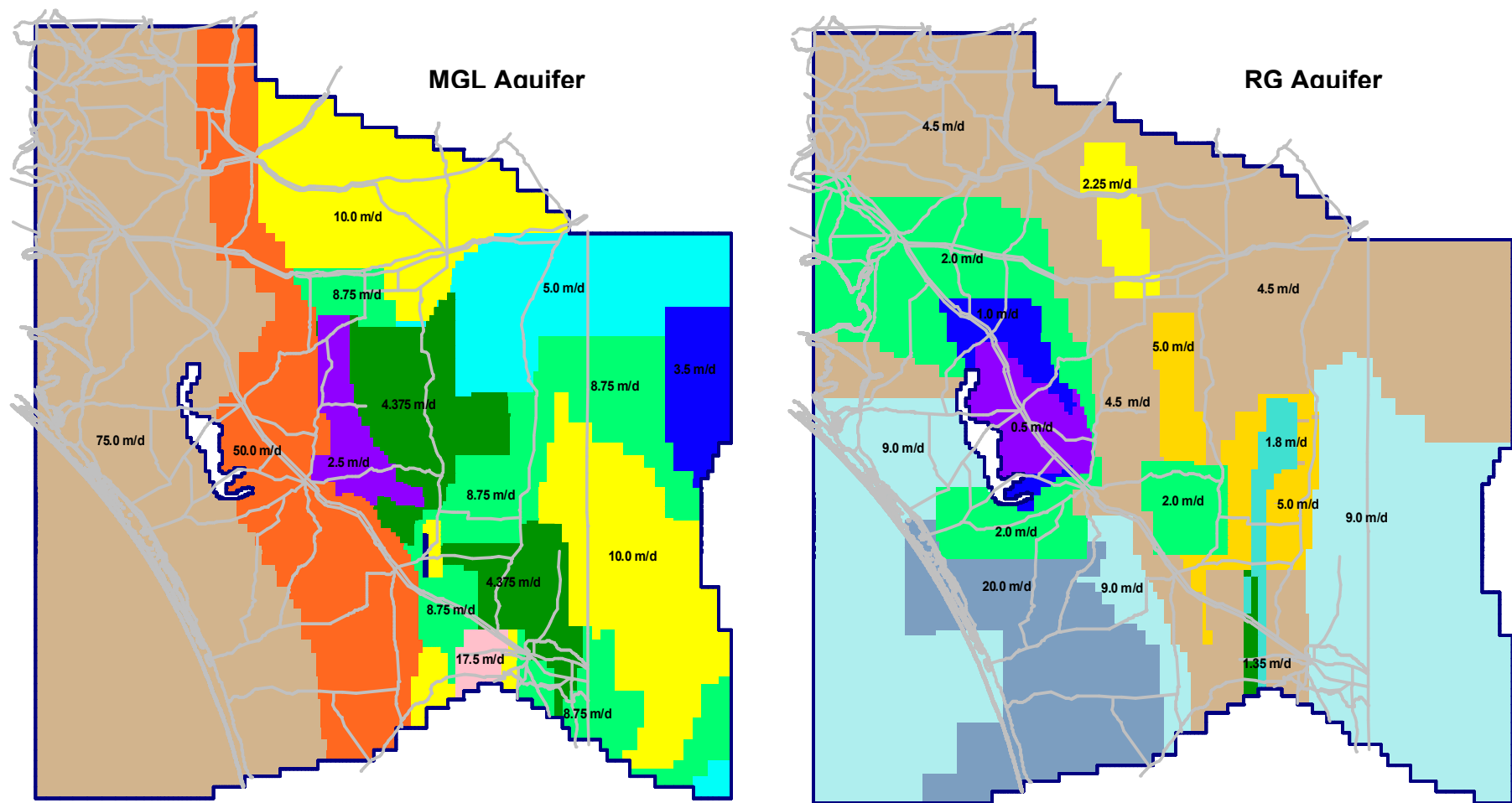


Figure 11 Calibrated horizontal hydraulic conductivities for the MGL and RG aquifers

Table 4 Summary statistics for simulated horizontal hydraulic conductivity

Model layer	Hydrogeologic unit	Simulated horizontal hydraulic conductivity, m/day				
		Median	Mean	Standard deviation	Minimum	Maximum
Layer 3	MGL	8.75	23.23	25.92	2.25	75.00
Layer 4	Ettrick Marl	5e ⁻⁰⁰⁵	1e ⁻⁰⁰⁵	5e ⁻⁰⁰⁵	1e ⁻⁰⁰⁵	5e ⁻⁰⁰⁵
Layer 5	RG	4.50	5.00	3.90	0.50	20.00

SENSITIVITY ANALYSIS

To help assess the importance of the uncertainty associated with the parameters used in the model, a sensitivity analysis was conducted on those parameters that were adjusted during the calibration process. Sensitivity analysis was made on 4 data sets calibrated in the steady state model: recharge, aquifer horizontal hydraulic conductivity, aquifer vertical hydraulic conductivity and confining bed vertical hydraulic conductivity. Four data sets, storage coefficient, aquifer horizontal hydraulic conductivity, aquifer vertical hydraulic conductivity and confining bed vertical hydraulic conductivity were tested in the transient state (1960 – 1997) model.

The sensitivity was measured by varying the model input through increments both greater than and less than each of calibrated parameters, and observing the resultant change in statistical error (steady state) and in simulated hydraulic head (transient simulation). Each parameter was tested independently of the others. The results of the sensitivity testing illustrated how the model performed using alternative input values, as opposed to the calibrated input.

Steady state sensitivity analysis

The sensitivity of the model in steady state was determined during predevelopment by varying calibrated values of aquifer hydraulic conductivities, and the vertical conductivities of confining beds and recharge. The effects of varying the steady state calibrated input values were expressed in terms of changes in the three statistical errors, as shown in Table 5 and Figure 12.

The steady state model of predevelopment conditions is less sensitive to increases in both horizontal and vertical hydraulic conductivity values than to decreases. The steady state model is most sensitive to decrease in horizontal hydraulic conductivity (Fig 12). A decrease in aquifer horizontal hydraulic conductivity by a factor of four increased the Root Mean Square Error value from 0.149 to 48.881 m (Table 5).

Table 5 Sensitivity analyses with respect to horizontal hydraulic conductivity

Error (m)	Multiples of horizontal hydraulic conductivity				
	0.25	0.5	1.0	1.5	2.0
Mean error	46.06	15.49	-0.062	-5.78	-8.91
Absolute mean error	46.06	15.49	0.127	5.78	8.91
Root mean square error	48.89	16.37	0.149	6.14	9.48

	Multiples of vertical hydraulic conductivity					
	0.1	0.5	1.0	1.5	2.0	3.0
Mean error	0.19	0.11	-0.062	-0.07	-0.12	-0.18
Absolute mean error	1.52	0.31	0.127	0.19	0.26	0.36
Root mean square error	2.07	0.40	0.149	0.26	0.37	0.50

	Multiples of recharge						
	0.1	0.25	0.5	1.0	1.5	1.2	2.25
Mean error	-18.47	-15.11	-9.80	-0.062	9.16	3.72	22.78
Absolute mean error	18.47	15.11	9.80	0.127	9.16	3.72	22.78
Root mean square error	19.69	16.11	10.44	0.149	9.77	3.96	24.34

When the input parameters are less than the calibrated values, horizontal hydraulic conductivity is very sensitive, followed by recharge and vertical hydraulic conductivity. When input parameters are higher then the calibrated values, recharge is very sensitive followed by horizontal hydraulic conductivity and vertical hydraulic conductivity. Of the three parameters tested, vertical hydraulic conductivity is the least sensitive.

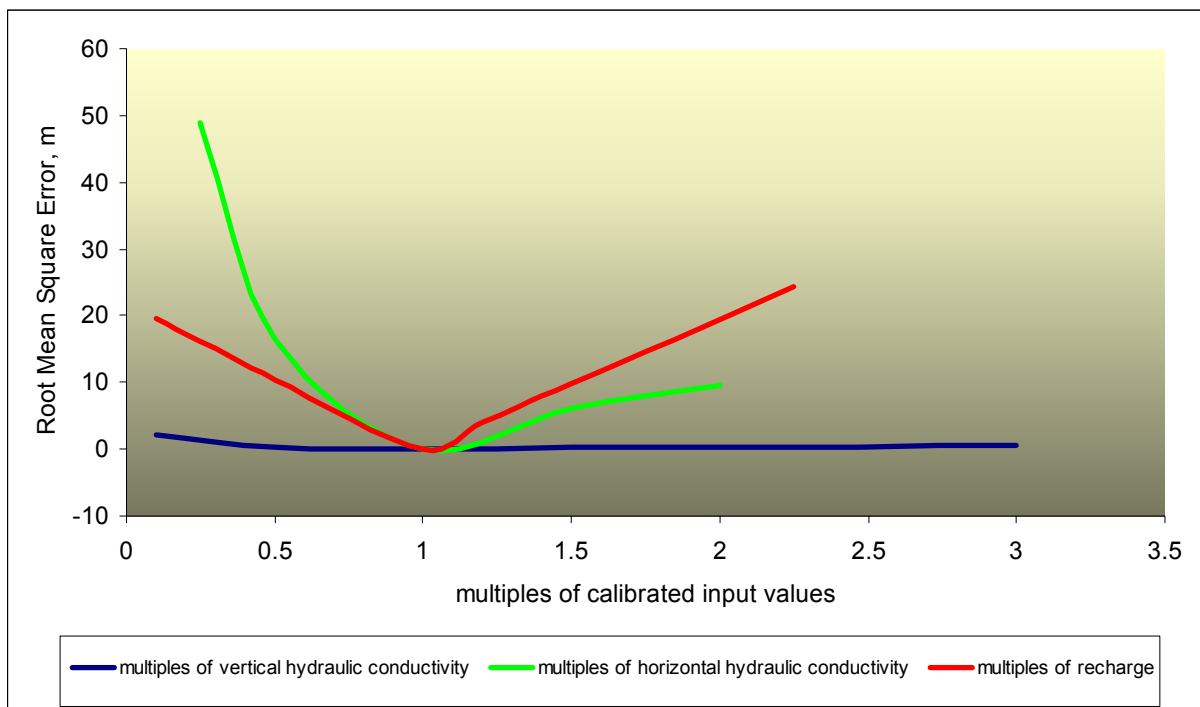


Figure 12 Sensitivity analysis

TRANSIENT MODEL CALIBRATION

The transient model, which was simulated by using the steady state results as the initial condition, started from predevelopment (April 1960) to September 2004. The transient simulation was divided into two stages. The first stage, which was run from 1960/61 through to 1996/97, was used to calibrate the model. The second stage was run from 1997/98 through to 2003/04 and was used to validate the model. The transient model was calibrated and validated to changes in water levels in response to recharge and pumping.

Each year was divided into two stress periods representing summer and winter. The winter stress period began in April and lasted for 155 days. The summer stress period, which began in September, is made up of 210 days. These stress periods were selected to almost coincide with pumping and recharge periods and to the times during which water levels in wells in the observation networks were measured. It was assumed that there is no groundwater pumping during winter periods. The summer and winter stress periods were divided into 7 and 5 time steps, respectively. The time units were days.

During the transient calibration, adjustments were made to the aquifer specific yield and specific storage values within reasonable limits to achieve an acceptable match between the calculated and measured water levels. Figure 13 shows the location of observation wells located within or close to the study area, while Figures 14 - 16 show the comparison between the transient results and the observed hydrographs.

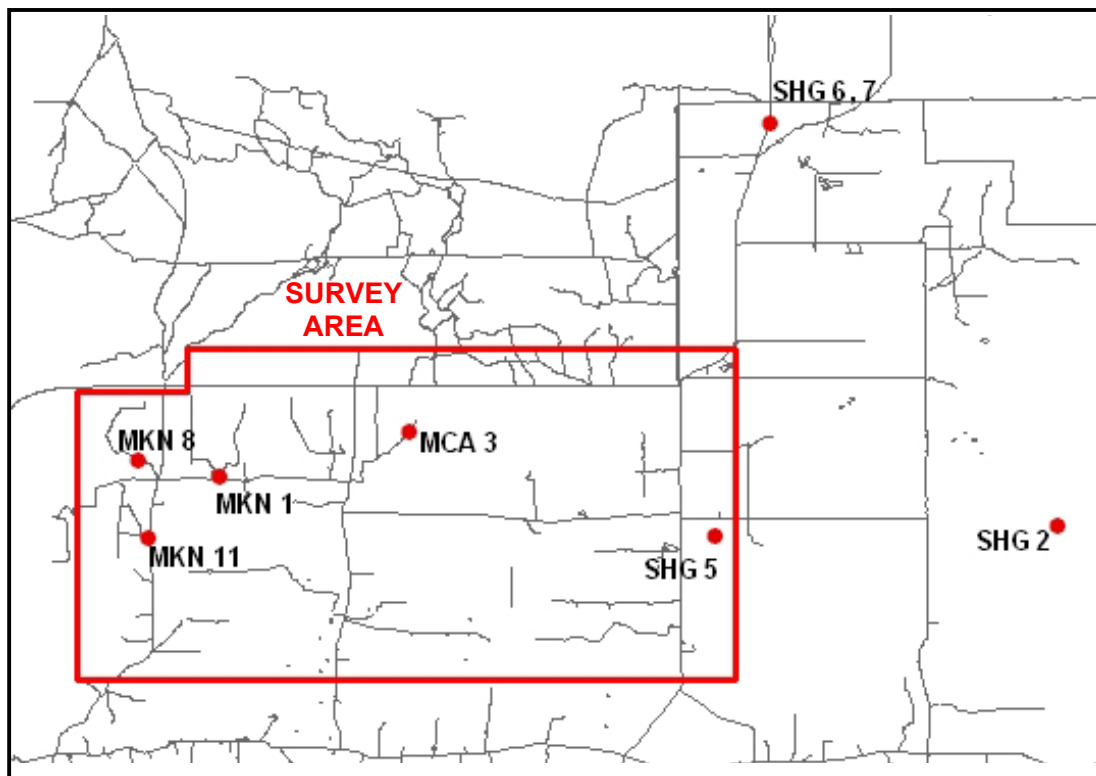


Figure 13 Location of observation wells in study area

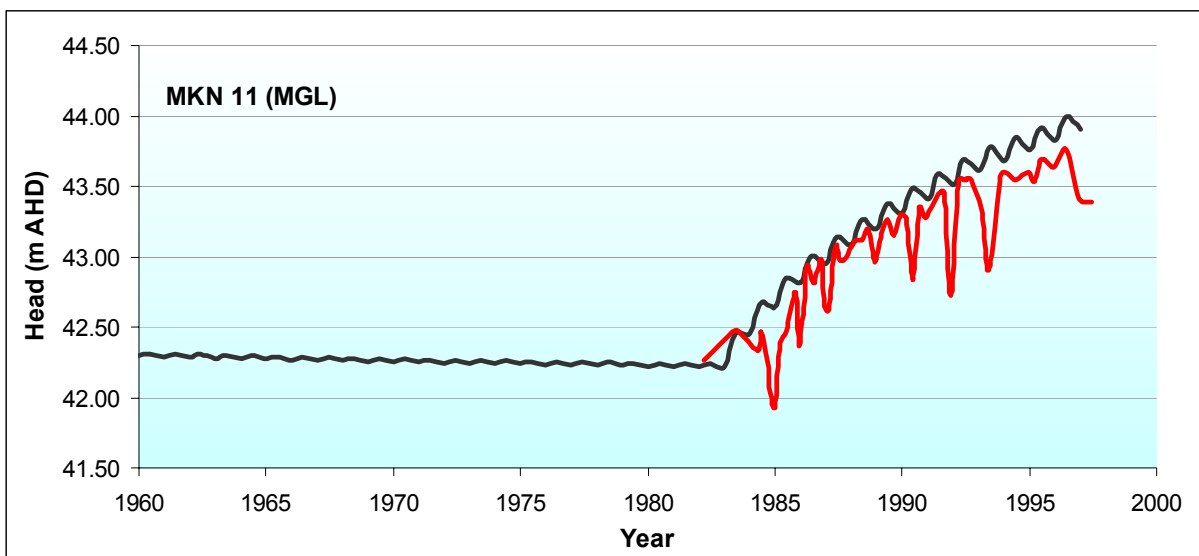
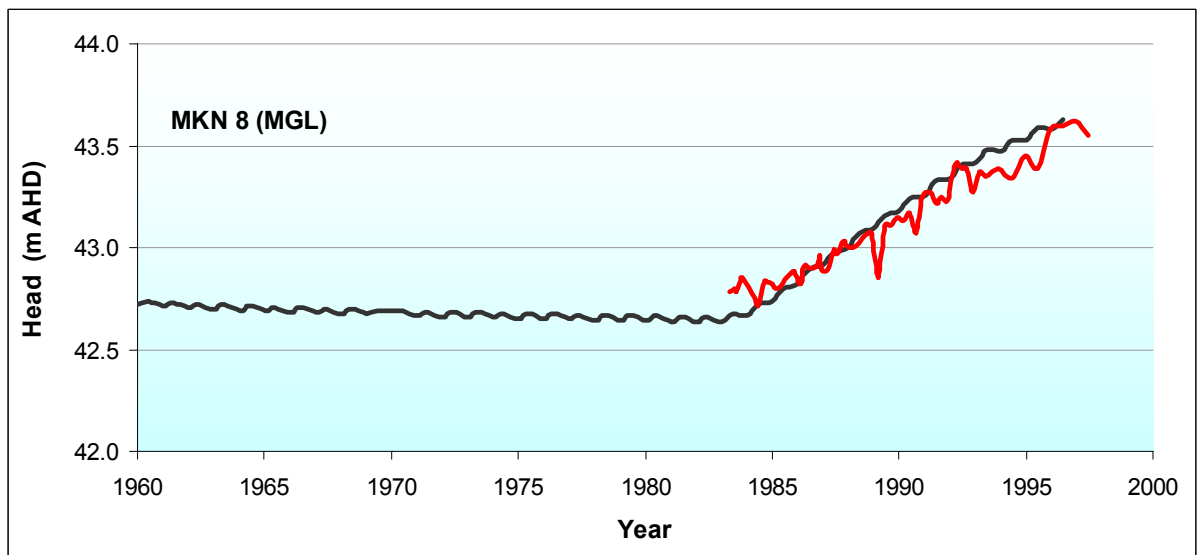
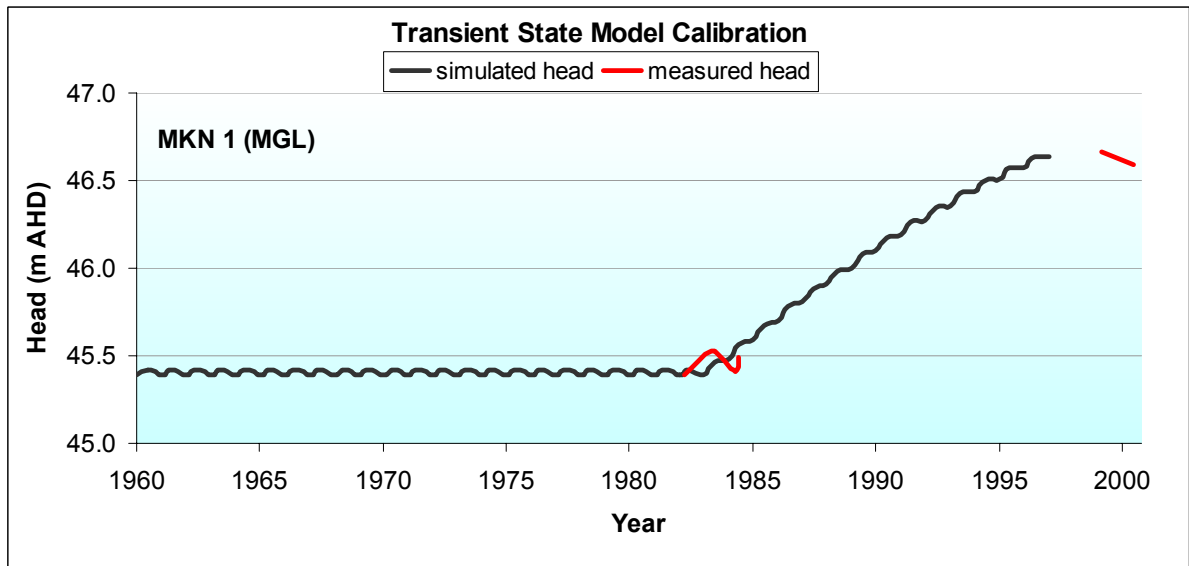


Figure 14 Comparison between simulated and measured transient conditions – Bores
MKN 1, 8, and 11

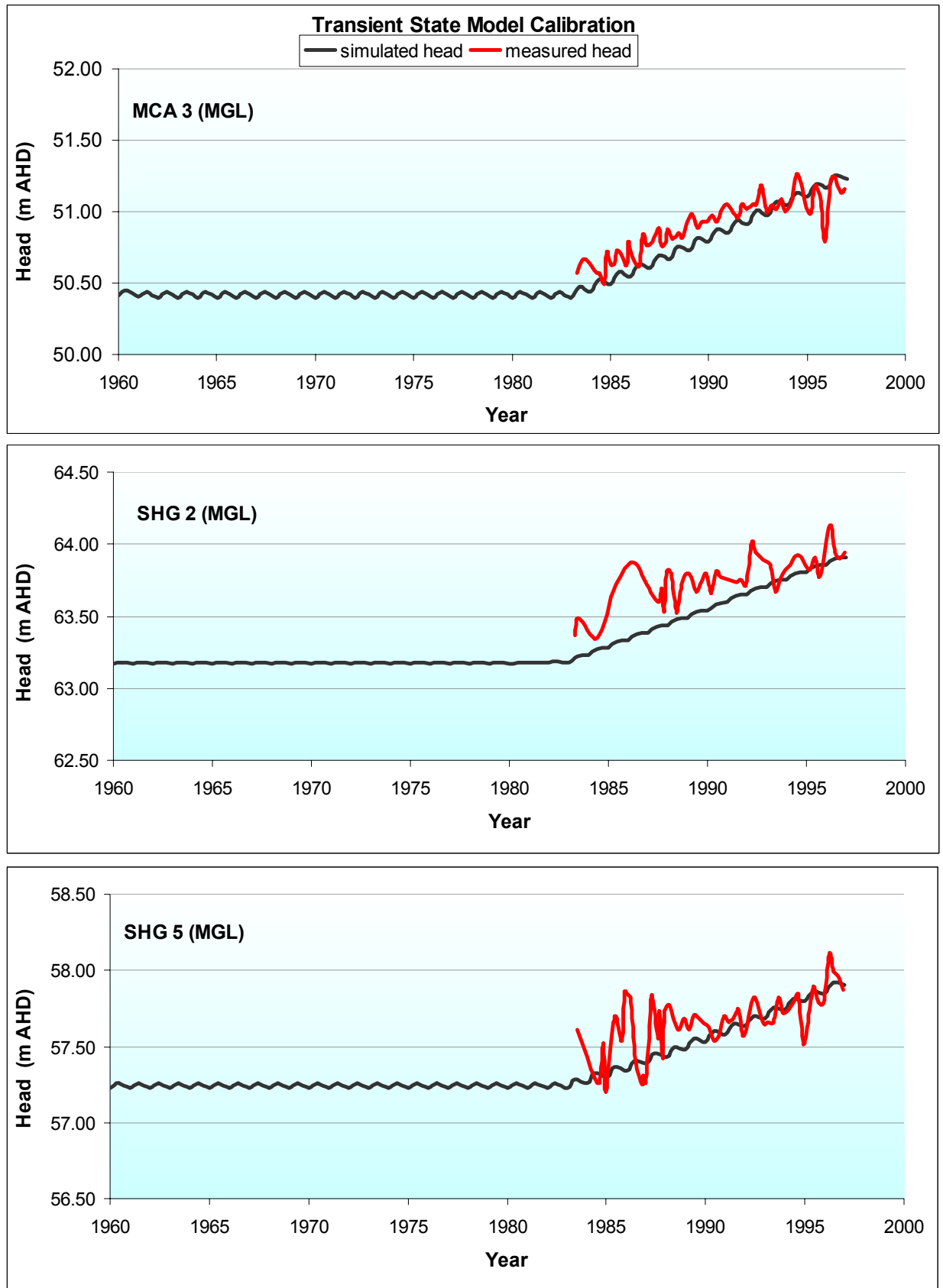


Figure 15 Comparison between simulated and measured transient conditions – Bores
MCA 3, SHG 2 and 5

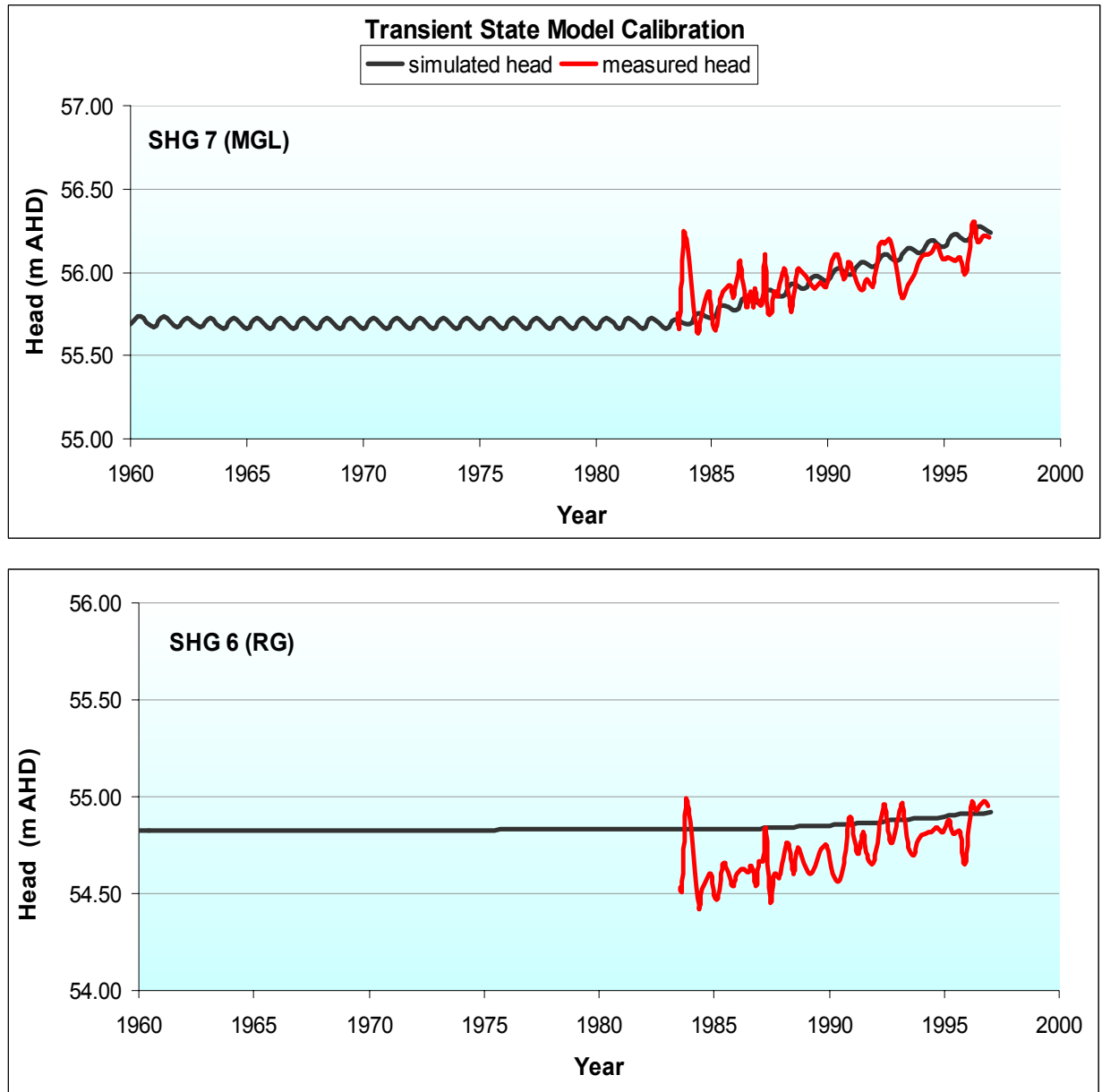


Figure 16 Comparison between simulated and measured transient conditions – Bores SHG 6 and 7

A satisfactory match between simulated and measured transient conditions was obtained when specific yield values ranging from 0.08 and 0.18 were used for the MGL aquifer, and specific storage values of $1e^{-5}$ to $8e^{-5}$ 1/m used in RG aquifer (Fig 17).

The transient calibration was not evaluated on the basis of Mean Error, Mean Absolute Error and Root Mean Square Error calculations, but inspection of the simulated versus observed hydrographs data (Figs 14 - 16) show that the transient model simulated head data that compares well to heads measured between 1983 and 1997. The differences between the simulated and observed heads may be due to several factors, including the large time steps and large grid size used in the model, the limited ability of the model to simulate steeper hydraulic gradients that occur near pumping wells, and the inaccurate estimates of extraction rates (meters are only just being installed).

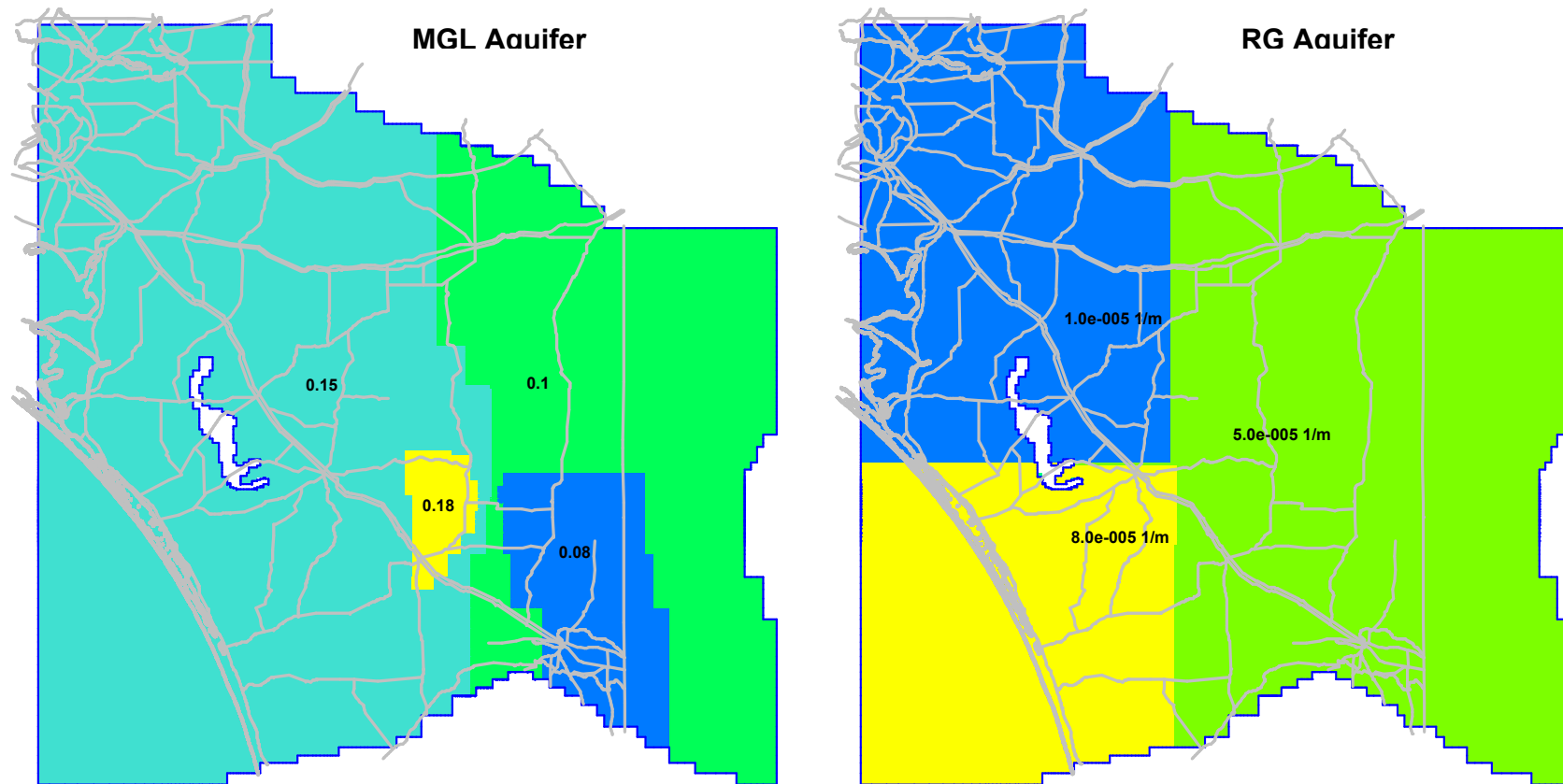


Figure 17 Calibrated values of specific yield (MGL) and storativity (RG)

Limitations of space and time should be noted when evaluating the transient model. The model-simulated hydraulic heads represent relatively long term conditions over large areas (cell size), whereas the field-measured heads may include short term, local effects of pumping and recharge. In reality, the pumping rates and recharge may vary during a given stress period, but in the transient simulation, recharge and pumping rates were kept constant for the duration of the stress period. Owing to these considerations, the differences between the observed and simulated heads are acceptable.

MODEL VALIDATION

Following calibration and sensitivity analysis, the calibrated model was tested against measured water level data that were not used in the calibration process. The calibrated model was used to reproduce 1997 to 2004 measured water levels at observation points under historic field conditions (Figs 18, 19). The seven year history matching of the measured water level at the observation wells show that the model overpredicts (i.e. overestimates) the groundwater levels. Apart from observation well MKN001 where the model greatly over predicted the water level (the difference is more than 1.0 m), the difference at the remaining observation sites are not greater than 0.3 m.

The probable cause for the differences between the measured and predicted water levels is, among other factors, inaccurate groundwater pumping rates used in the simulation. Taking into account measurement errors and likely inaccurate pumping rates, the predictive capability of the flow model can be said to be reasonable and fairly accurate, and can be used for predicting water levels with reasonable confidence. This assurance does not, however, extend to conditions other than those tested and does not account for unforeseen stresses. The validation results show how the model can simulate past conditions, but it does not necessarily indicate the accuracy for future predictive simulations.

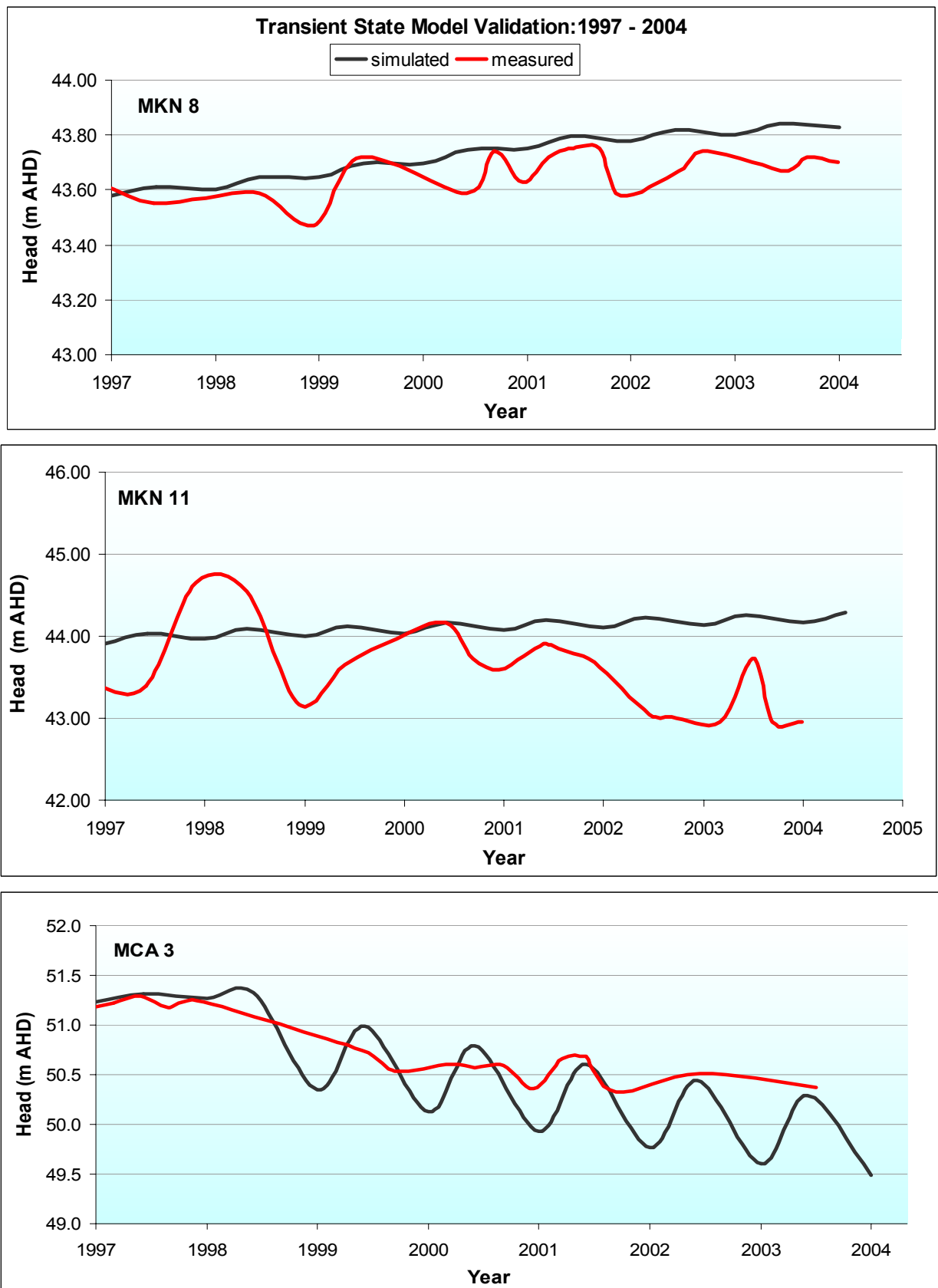


Figure 18 Comparison between simulated and measured validation conditions – Bores
MKN 8 and 11, MCA3

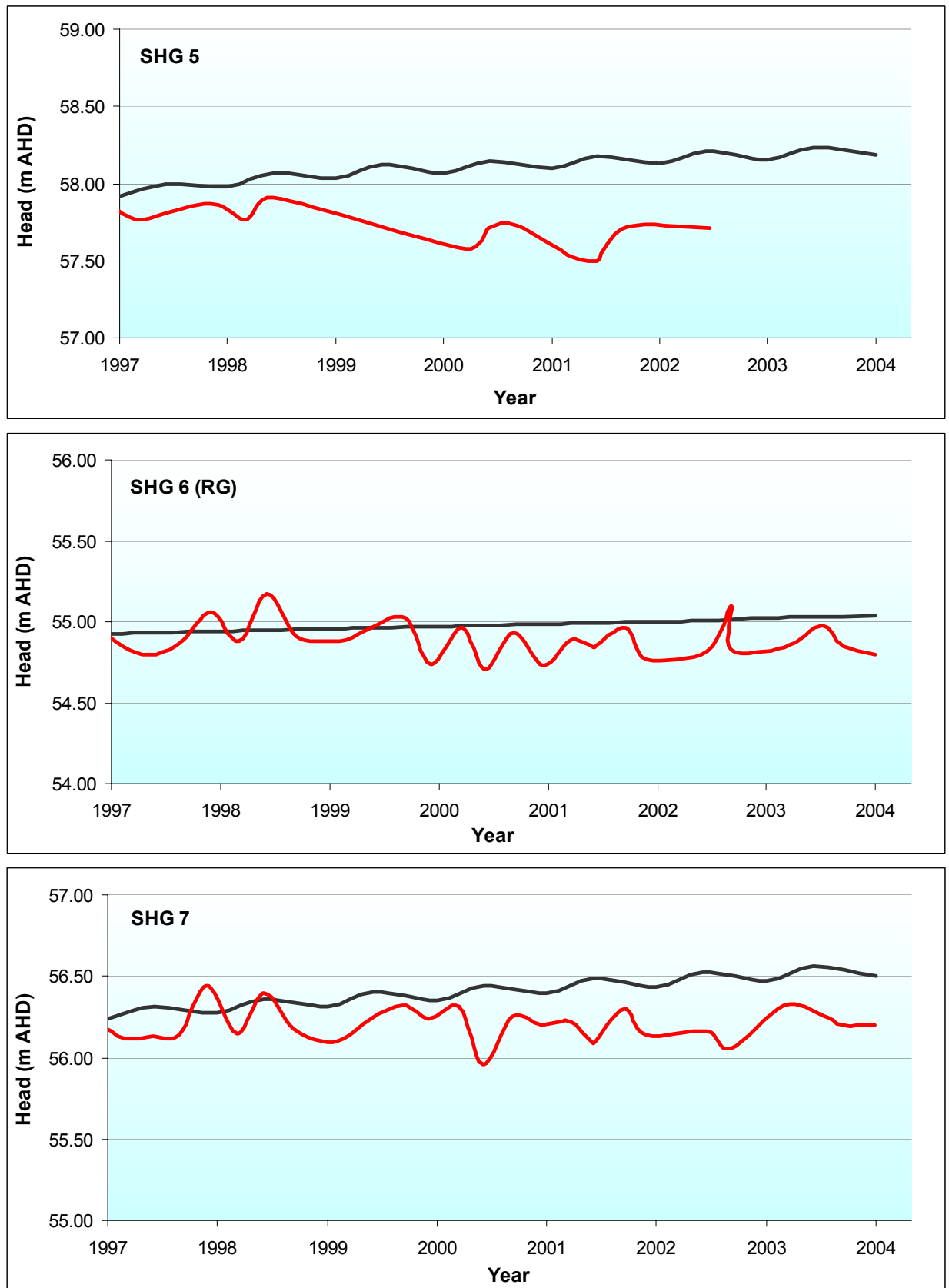


Figure 19 Comparison between simulated and measured validation conditions – Bores
SHG 5, 6 and 7

SALT LOAD MODELLING

Model development and calibration

MT3D was used to simulate changes in groundwater salinity as a result of the flushing of unsaturated zone salt to the watertable following clearing. MT3D is a program designed to model contaminant transport based on a pre-solved groundwater flow model (MODFLOW was used to solve the ground water flow equations). MT3D can be used to simulate changes in concentrations of soluble components in groundwater taking into account advection, dispersion, diffusion and simple chemical reactions, with various types of boundary conditions and external sources or sinks. The model can accommodate very general spatial discretization schemes and transport boundary conditions, including:

- 1) confined, unconfined or variably confined/unconfined aquifer layers;
- 2) inclined model layers and variable cell thickness within the same layer;
- 3) specified concentration or mass flux boundaries;
- 4) the transport effects of external hydraulic sources and sinks such as wells, drains, rivers, areal recharge and evapotranspiration.

A uniform effective porosity value was assigned to the model layers because no data were available to determine the spatial distribution of porosity. The effective porosity of the MGL aquifer was set at 10 %. The values of longitudinal dispersivity, transverse dispersivity and vertical dispersivity were assumed to be 17.5 m, 1.75 m and 1.0 m respectively. These values meet gridding stability criteria recommended by Pickens and Griskak (1981), Gelhar (1992) and ASTM (1995).

The MT3D model extent covers the study area only, and not the whole GMS model area.

Data availability for the computer model

The following data were used:

- Observed salinity hydrographs (TDS) from five observation wells in the study area
- Salinity contour map representing steady-state salinity condition (Fig 20)
- Recharge and salt flux data sourced from Leaney et al (2004)
- Current (2000/01) groundwater extraction data

The salinity concentration of the recharge (in mg/L) was obtained dividing the salt flux by the recharge rate.

Boundary conditions

The boundary conditions used in the transport modelling included constant concentration and no-transport boundaries. The constant concentration and no-transport boundaries coincided with the constant head and no-flow boundaries used in the flow model.

Calibration of the salinity model

Calibration was aimed at the determination of the dispersion parameters with no prior estimation. These were longitudinal dispersivity, the ratio of transverse dispersivity to longitudinal dispersivity, and the ratio of vertical dispersivity to longitudinal dispersivity. The initial values of the dispersion parameters were selected from the literature and applying the rule-of-thumb principle (Gelhar 1992, ASTM 1995, EPA 1986).

STEADY STATE TRANSPORT SIMULATION

To produce a reasonable concentration distribution as initial conditions for the transient state salt flux simulations, a steady state MT3D simulation was run. During the steady state calibration run, the initial transport parameters obtained from the literature were adjusted until an acceptable match to salinity concentrations observed in 1983 at the five monitoring sites was achieved. The steady state calibration involved the simulation of rainfall recharge and rainfall recharge concentration, which was assumed to be 300 mg/L.

The result of the steady state run showing a steady-state concentration distribution is shown in Figure 20. Concentrations at monitoring well locations were also compared with simulated concentration in Table 6 and Figure 21.

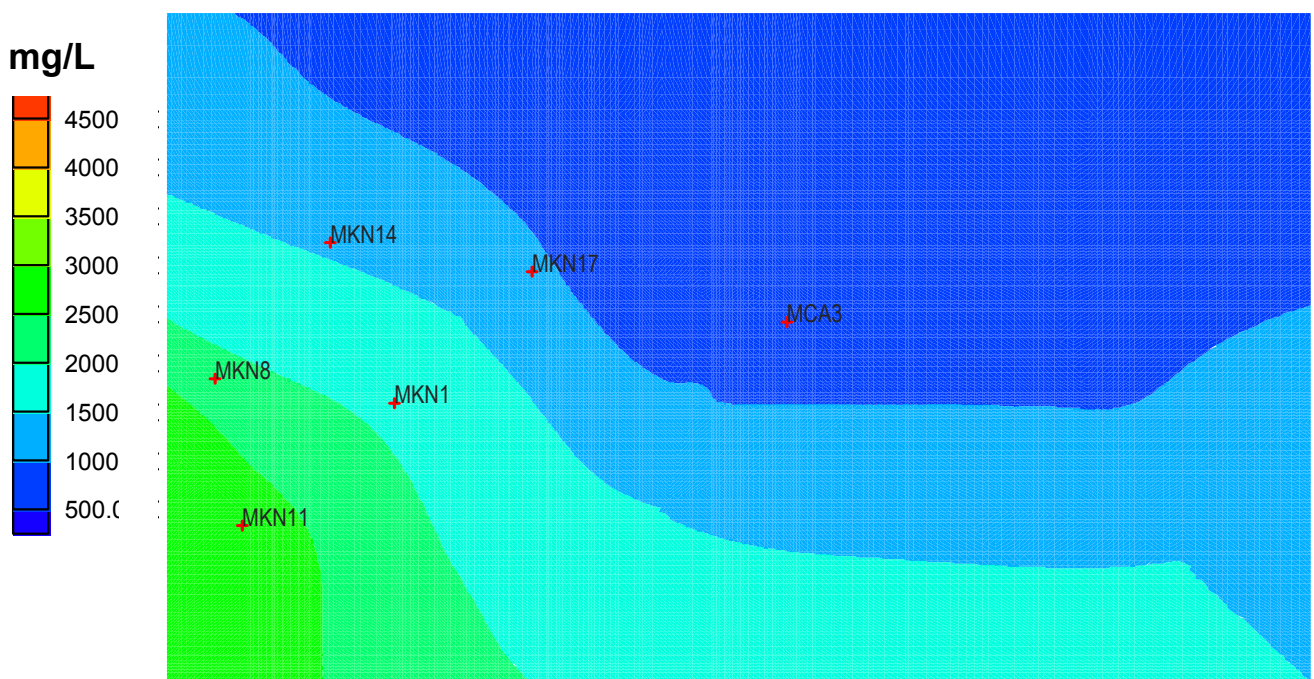


Figure 20 Steady-state simulated salinity contours

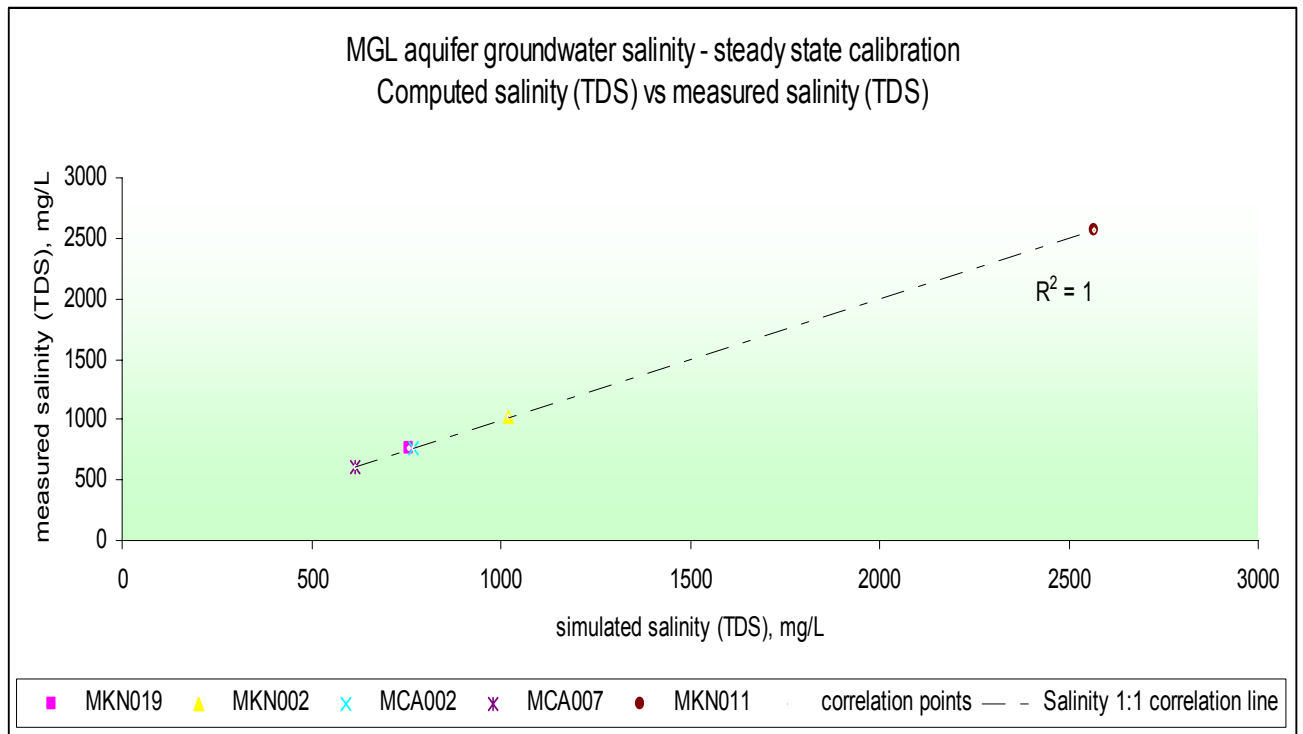


Figure 21 Steady-state simulated salinity contours

Table 6. Comparison of measured and calculated salinity

Observation well	Aquifer monitored	Location		Initial salinity (mg/L)		
		Easting	Northing	Measured	Calculated	Residual
MCA002	MGL	465205	6022154	770	770.20	0.20
MCA007	MGL	470920	6022809	614	614.37	0.37
MKN002	MGL	463045	6019959	1021	1021.45	0.45
MKN011	MGL	453283	6017399	2567	2569.98	0.01
MKN019	MGL	461700	6023249	757	758.04	1.04

Table 7 gives the calibrated transport parameters of the MGL aquifer. All the transport parameters shown in this table are reasonable for the type of geologic material, solute and cell size. The calibrated longitudinal dispersivity is 17.5 m; horizontal dispersivity is 1.75 m; vertical dispersivity is 0.00875 m; and diffusion coefficient is $1.75 \times 10^{-4} \text{ m}^2/\text{d}$. The calibrated value represents that of Cl^- , which is conservative.

Table 7. Transport parameters used in model calibration

Parameter	Value
Longitudinal dispersivity, (m)	17.5
Ratio of transverse dispersivity to longitudinal dispersivity	0.1
Ratio of vertical dispersivity to longitudinal dispersivity	0.0005

Effective molecular diffusion coefficient, (m ² /d)	1.75e-005
Effective porosity	0.1

TRANSIENT STATE TRANSPORT CALIBRATION

Using the calibrated steady-state salinity simulation results as a starting salinity distribution, a series of unsteady state simulations were carried out to fit the measured and simulated salinity concentration data at the five monitoring sites over the period of 1983 to 2004. Calibration of the transient model was done by comparison of model simulated and measured groundwater salinity concentration data from five monitoring wells in the MGL aquifer in the study area. The transient calibration involved the simulation of pumping, recharge of rainfall and recharge of salt load in excess irrigation water.

The simulated salinity distribution in the MGL aquifer is reasonably consistent with the field-measured data as shown in Figures 22 and 23. A comparison between measured and calculated salinities is presented in Table 8. Based on these data, it can be said that the actual groundwater salinity (TDS) concentration at these monitoring points does not differ from the simulated values.

Table 8. Comparison of measured and calculated salinity - April 2003

Observation well	April 2003 salinity (mg/L)		
	Measured	Calculated	Residual
MCA002	799	797	-2
MCA007	680	649	-31
MKN002	1066	1054	-12
MKN011	2710	2533	-177
MKN019	1016	777	-239

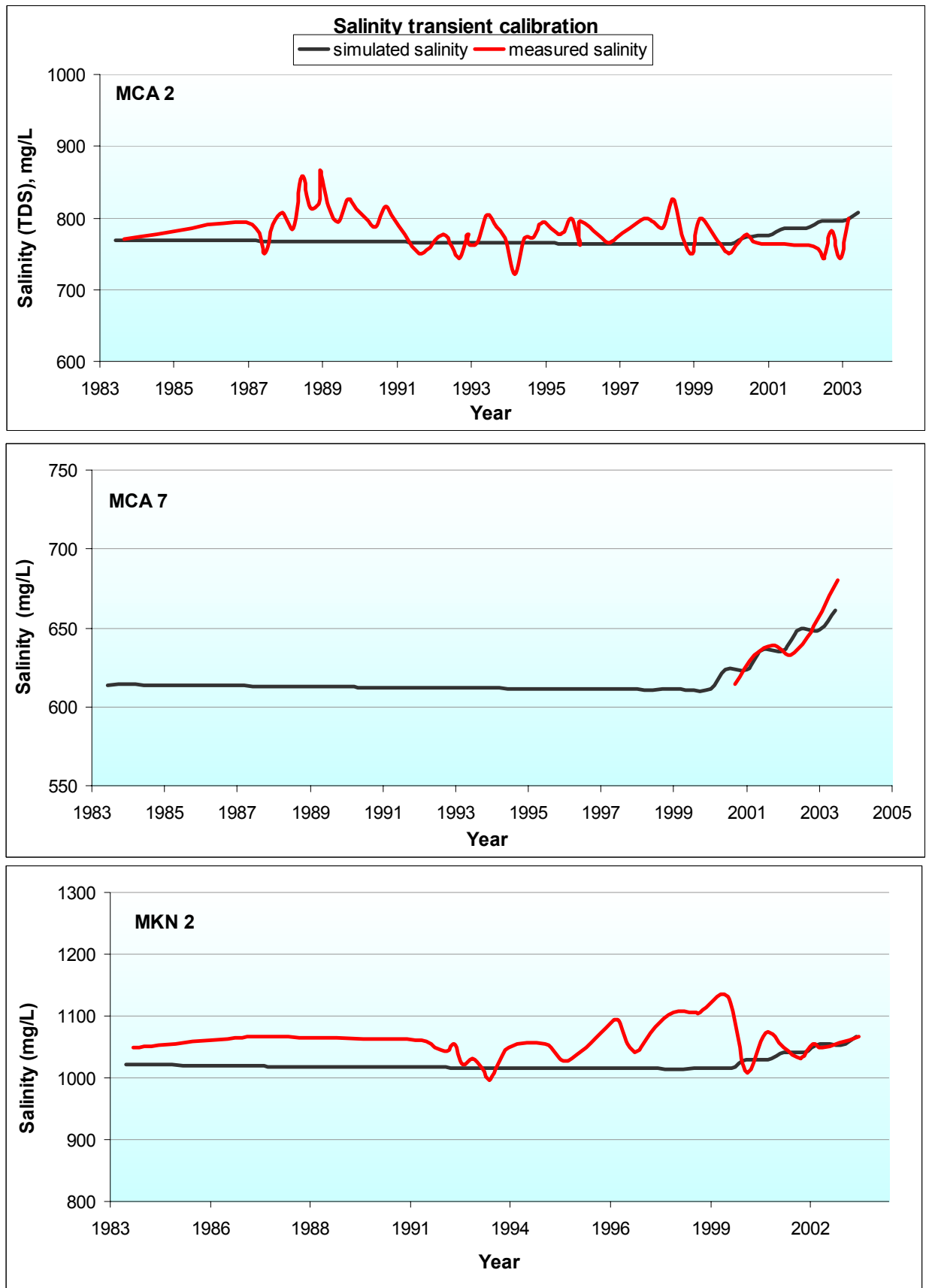


Figure 22 Comparison between simulated and measured transient salinity conditions –
Bores MCA 2 and 7, MKN 2

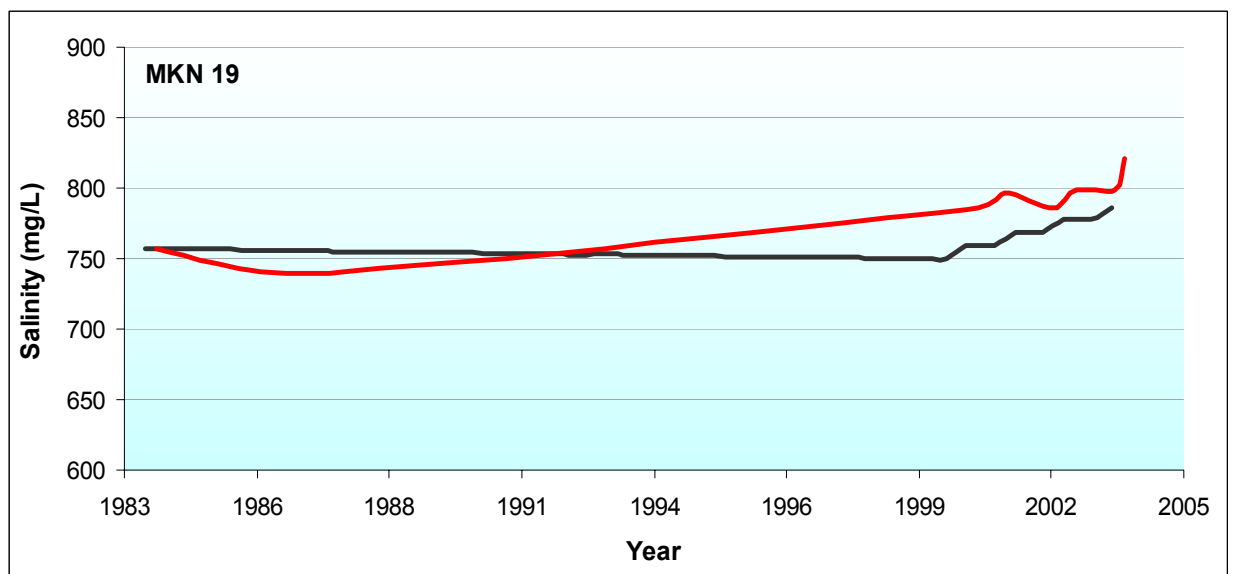
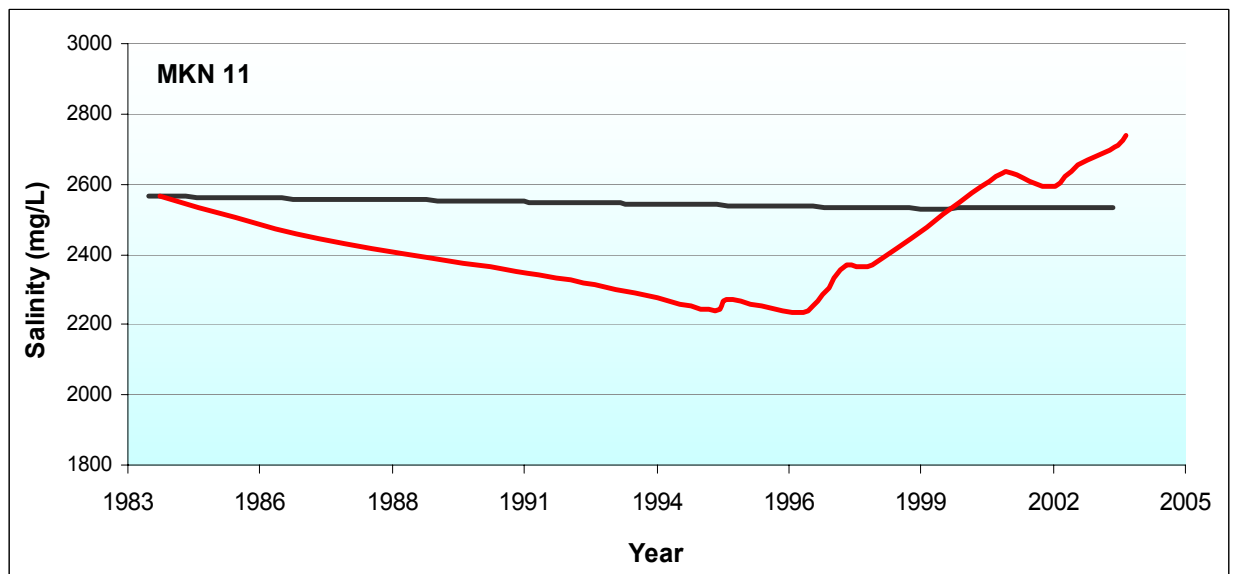


Figure 23 Comparison between simulated and measured transient salinity conditions – Bores MKN 11 and 19

SIMULATION OF GROUNDWATER SALINIZATION IMPACTS

Using the calibrated transport model and starting with 2004 simulated salinity (TDS) concentration, the salinity response of the MGL aquifer to the flushing of unsaturated zone salt was investigated. The salinity concentration in the salt load was sourced from Leaney et al (2004). Both dryland farming and summer irrigation conditions were simulated.

The following assumptions were made.

- The primary source of salt was from the unsaturated zone lying above the water table in the MGL aquifer
- During winter periods, the entire area of the study site was simulated as potential source of salt and winter rainfall was simulated as the potential source of recharge
- Irrigation commenced in 1993, and at some sites, was carried out every four years to simulate the crop rotation used for vegetable irrigation
- Through the summer months only, the irrigation sites were simulated as potential sources of salt and return flow from irrigation drainage water
- A continuous source of salt flushing to the groundwater was created by assigning constant salinity concentration and recharge to the topmost active cells
- For each stress period, constant concentration and recharge values reflecting field determined salt flux and recharge values were assigned to the model grid
- The salt concentration and recharge in the unsaturated zone were updated at regular intervals during the simulation (1993, 2004 and 2054)
- The salt mass was advected and/or dispersed away from the water table into the groundwater

Dryland simulation

Figure 24 shows the predicted changes in groundwater salinity in the MGL aquifer at five observation points in the study area in response to flux of salt from non-irrigated dryland areas. The model results indicate a sharp increase in most of the bores after 2050 approximately, which indicates the arrival of the salt front at the watertable. Table 9 details the rate of increase in groundwater salinity in the MGL aquifer from 2050 to 2100 which varies from 15 – 30 mg/L/yr. Variations in the salinity at these sites before 2050 is mostly due to the lateral movement of groundwater in a westerly direction under natural gradients.

Table 9 Comparison of 2004 and 2100 simulated salinity

Observation well	Simulated 2004 salinity (mg/L)	Simulated 2050 salinity (mg/L)	Simulated 2100 salinity (mg/L)	Rate of increase 2050 - 2100 (mg/L/yr)
MCA002	902	811	2271	29.2
MCA007	665	767	1500	14.6
MKN019	980	920	2362	28.8
MKN002	1067	1413 (2070)	1984	19.1
MKN011	2905	3127 (2040)	5800	44.5

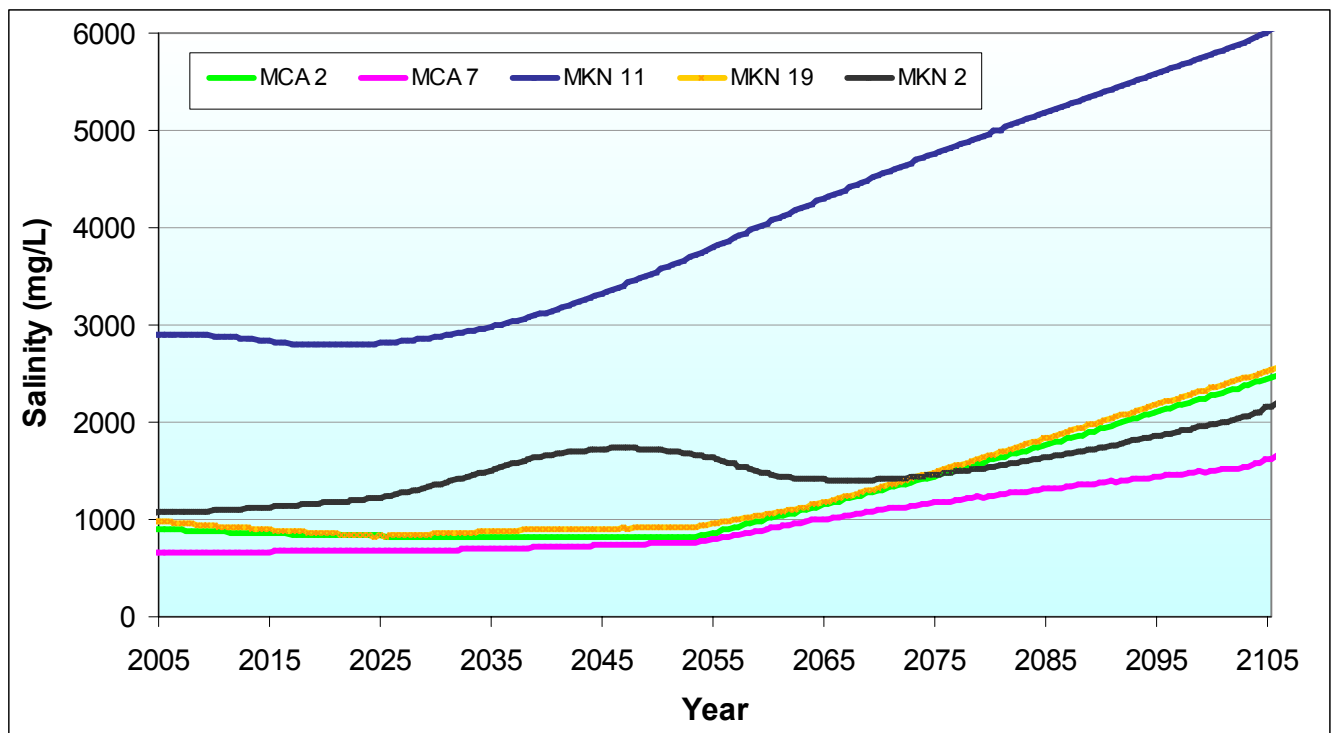


Figure 24 Modelled salinity predictions at five observation bores

Bore MKN 11 shows an earlier response than other bores, probably due to higher recharge rates in the area resulting from sandy soils and a shallower depth to watertable.

Figure 25 shows the simulated salinity concentration distribution in the MGL aquifer for the years 2004, 2050 and 2100.

These increases in groundwater salinity will result in unsuitability for new vegetable irrigation (in areas not previously irrigated), in about 50 years time. Significant areas will not have groundwater suitable for domestic consumption in about 80 years, while lucerne irrigation in new areas and stock supplies will be able to be maintained indefinitely.

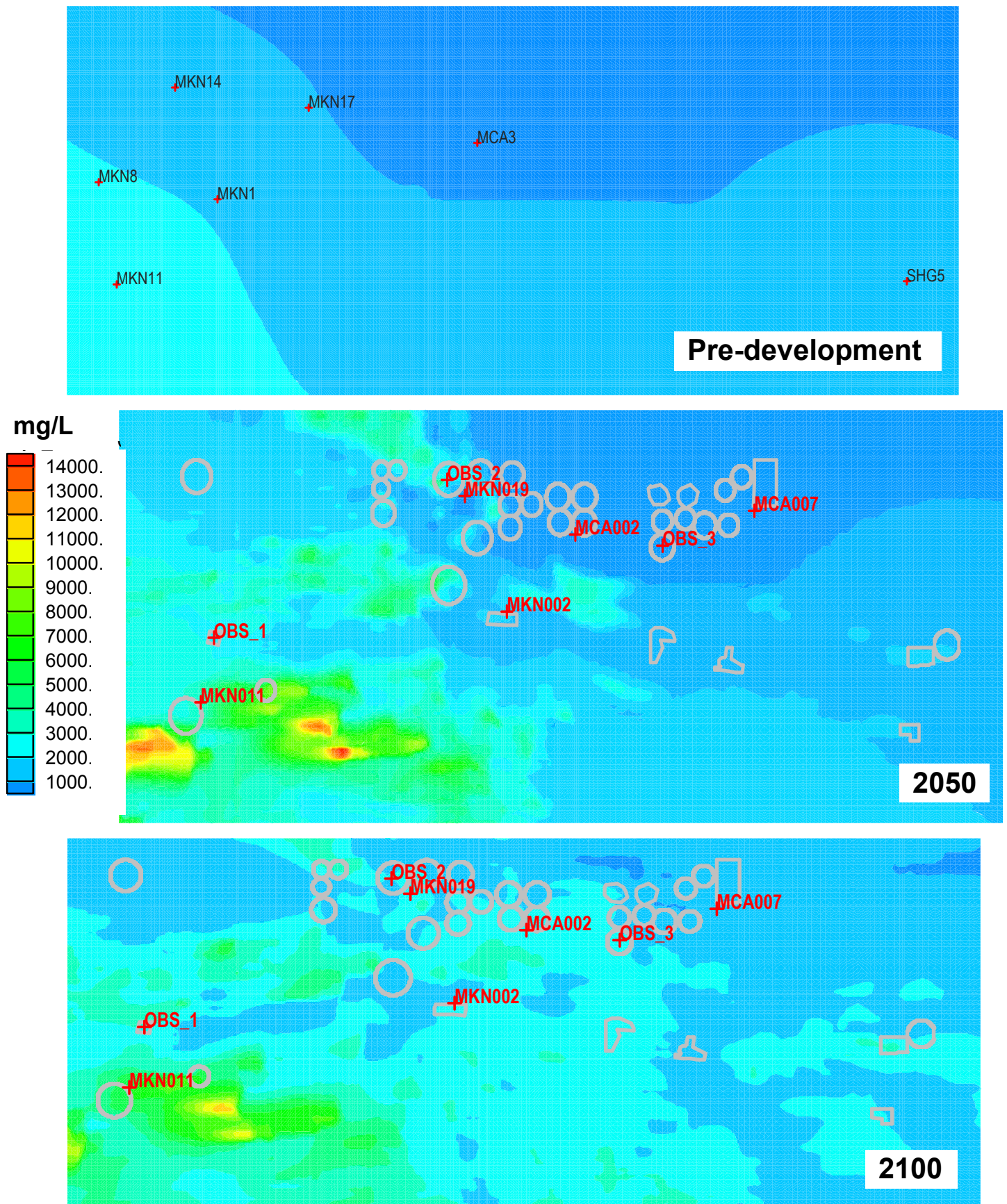


Figure 25 Modelled dryland salinity distribution in the MGL aquifer

Irrigation simulation

The changes in groundwater salinity under irrigated areas were simulated at two locations. OBS_2 was located within an area where summer irrigation is carried out every year, whereas OBS_3 is located where summer irrigation is applied to the land every four years to represent a vegetable rotation scenario. The location of these sites is shown in Figure 27. Figure 26 shows the changes in salinity with time at the two sites, with a comparison between dryland and irrigation scenarios at each site.

In both cases, irrigation has caused rapid rising of the unsaturated zone salt when compared with the dryland scenario. Irrigation at OBS_2 commenced in 1999 with rises in salinity detected in 2004. High drainage rates of 200 mm/yr have resulted in the complete flushing of the unsaturated zone salt store to the aquifer by 2050, with a resultant increase in aquifer salinity at an average rate of 183 mg/L/yr up to a maximum of 11 000 mg/L (if irrigation were to continue that long).

OBS_3 shows a similar but more gradual rising trend of 23 mg/L/yr over the 100 year period with no maximum reached. The drainage rate of 136 mm/yr was applied every four years, which accelerated the impact on aquifer salinity by about 50 years.

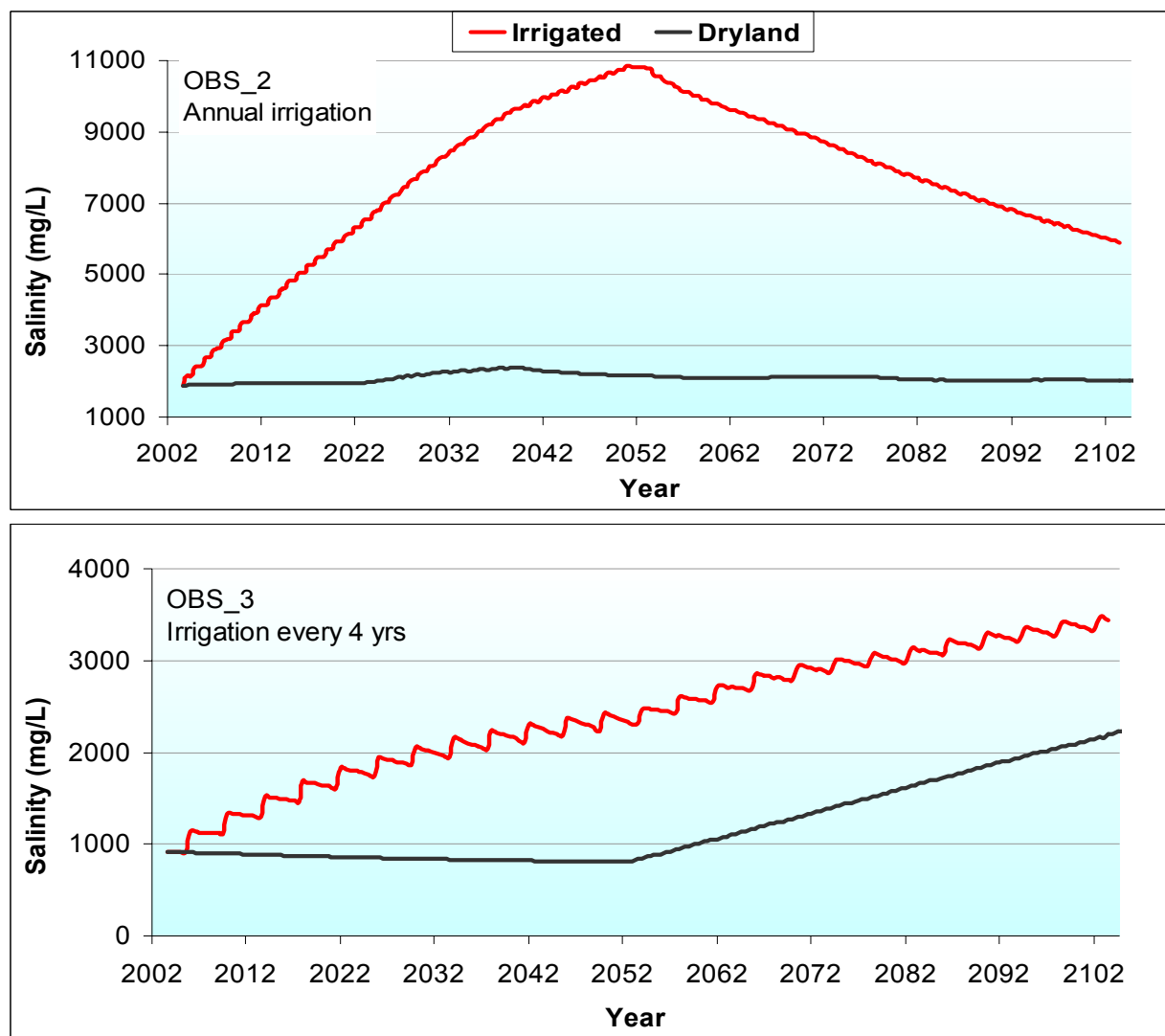
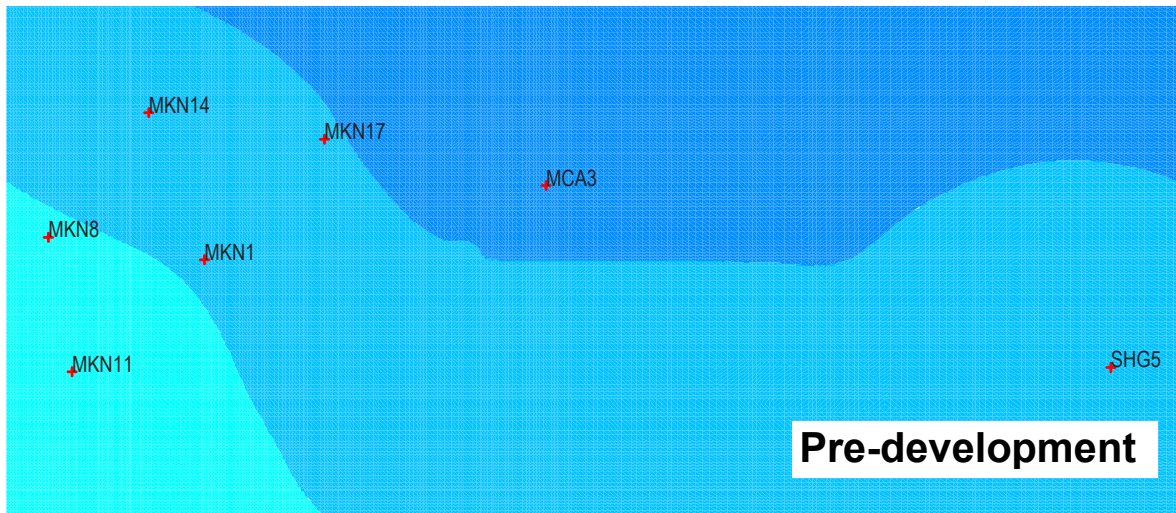


Figure 26 Modelled salinity predictions at two irrigated sites



mg/L

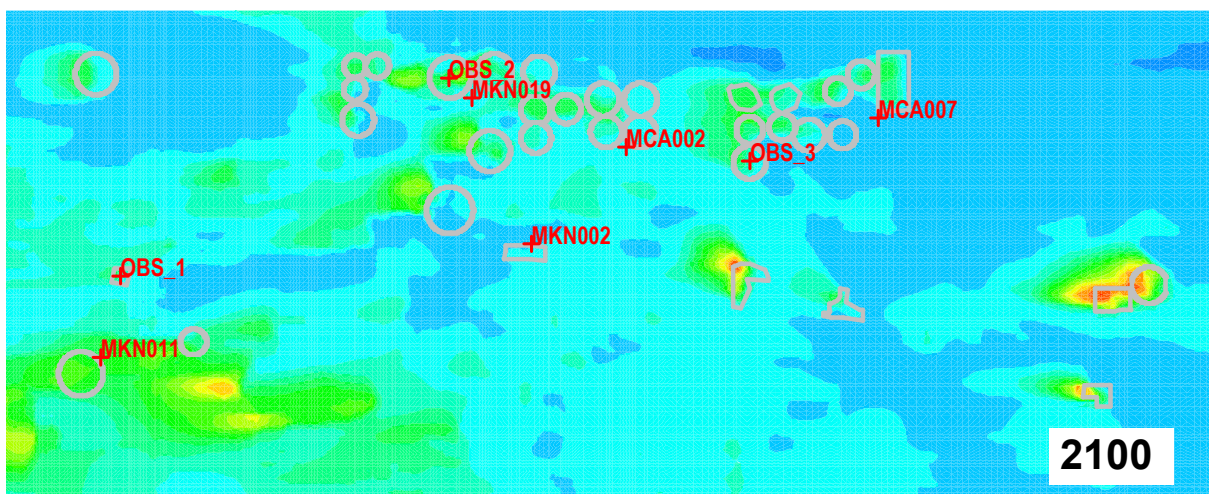
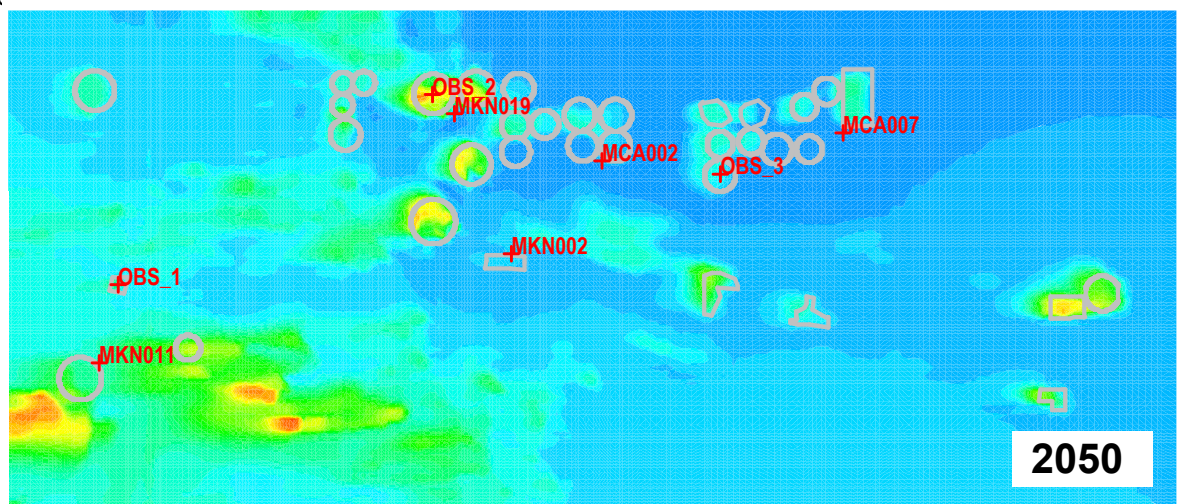
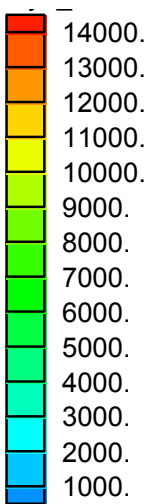


Figure 27 Modelled irrigated salinity distribution in the MGL aquifer

The areal salinity distribution showing the impacts of irrigation over time is shown in Figure 27. The areas of high recharge and sandy soils can be seen where salinities beneath irrigated areas have reached over 5000 mg/L by 2050 in the green and yellow areas. In reality, irrigation would have stopped as soon as salinities exceeded 3000 mg/L.

The movement of plumes of salinised groundwater in a westerly downgradient direction from beneath irrigated areas can also be seen in Figure 27. By 2050, the maximum distance of plume movement is about 500 m from beneath OBS_3. The direction of groundwater movement may be modified by pumping in some areas. This model may be used to refine the buffer distance currently enforced between new and existing irrigation.

CONCLUSIONS AND RECOMMENDATIONS

A calibrated groundwater flow and solute transport model has been constructed to predict the salinity impacts in the unconfined aquifer due to the flushing of unsaturated zone salt following clearing. Improved estimates of recharge rates and lag times before aquifer impact were used as inputs.

Under the dryland non-irrigation scenario, significant increases in aquifer salinity are expected to occur after 50 years from the present time. Rates of increase will vary from 15 – 45 mg/L/yr, depending on soil type. These increases in groundwater salinity will result in unsuitability for new vegetable irrigation (in areas not previously irrigated), in about 50 years time. Significant areas will not have groundwater suitable for domestic consumption in about 80 years, while lucerne irrigation in new areas and stock supplies will be able to be maintained indefinitely.

Beneath irrigated areas, the flushing of salt is accelerated markedly, with increases in salinity beneath the irrigated area beginning after only 10 years, with salinities too high for use after a further five years in areas of high recharge with sandy soils. Obviously, clayey soils and rotation of irrigated areas will delay salinity impacts by up to 30 to 40 years. After 50 years, the maximum lateral movement of salinised groundwater to the west from beneath the irrigated areas is about 500 m.

Before management strategies are investigated, salinity responses to varying irrigation drainage rates should be modeled to simulate the variation in irrigation efficiencies under different crop types.

Regular salinity monitoring of all irrigation bores and some dryland stock bores should be continued to help validate the model and better calibrate some parameters.

REFERENCES

- ASTM, 1995. Standard Guide for Risk-Based Corrective Action Applied at Petroleum Release Sites. American society for Testing and materials, ASTM Designation E 17390095.
- Barnett, S. R., 1991. Renmark Hydrogeological Map (1:250 000 scale). Bureau of Mineral Resources, Geology and Geophysics Canberra, Australia.
- Brigham Young University, 2000. The Department of Defense groundwater modelling system reference manual – GMS version 4.0. Provo, UT, Brigham Young University.
- Kellett, J. R., Evans, W. R., Allan, G. L., Davie, R. F. and Fifield, L. K., 1990. A study of stable chloride and chlorine-36 in the Murray Group Limestone, Western Murray Basin: *In* Proceedings of the International Conference on Groundwater in Large Sedimentary Basins.
- Lawrence, C. R., 1975. Geology, hydrodynamics and hydrochemistry of the southern Murray Basin. Mines Dept. Victoria, Australia.
- Leaney, F., Walker G., Knight, J., Dawes, W., Bradford, A., Barnett S. and Stadter, F., 1999. Potential for groundwater salinisation in Tintinara area of South Australia Impact of planned irrigation allocations. CSIRO Land and Water Technical Report 33/99.
- Leaney, F., Barnett S., Davies P., Maschmedt, D., Munday, T. and Tan K., 2004. Groundwater salinization in the Tintinara Highland area of SA: Revised estimates using spatial variation for clay content in the unsaturated zone. CSIRO Land and Water Technical report 24/04.
- McDonald, M. G. and Harbaugh, A. W., 1988. A modular three-dimensional finite-difference groundwater flow model, Techniques of Water-Resources investigations, Book 6, chapter A1, United States Geological Survey.
- Pickens, J. F., and Grisak, G. E., 1981. Modelling of scale-dependent dispersion in hydrogeologic system. Water Resources Research, vol 17(6): 1701 – 1711.